GEOCHEMICAL EVIDENCE FOR MICROBIALLY MEDIATED SUBGLACIAL MINERAL WEATHERING

by

Scott Norman Montross

A thesis submitted in partial fulfillment
of the requirements for the degree

of

Master of Science

in

Earth Sciences

MONTANA STATE UNIVERSITY
Bozeman, Montana

April 2007

APPROVAL

of a thesis submitted by

Scott Norman Montross

This thesis has been read by each member of the thesis committee and has been found to be satisfactory regarding content, English usage, format, citations, bibliographic style, and consistency, and is ready for submission to the Division of Graduate Education.

Mark L. Skidmore
(chair)

Approved for the Department of Earth Sciences

Stephan G. Custer

Approved for the Division of Graduate Education

Dr. Carl A. Fox

STATEMENT OF PERMISSION TO USE

In presenting this thesis in partial fulfillment of the requirements of a master's degree at Montana State University, I agree that the Library shall make it available to borrow under the rules of the Library.

If I have indicated my intention to copyright this thesis by including a copyright notice page, copying is allowable only for scholarly purposes, consistent with the "fair use" as prescribed in the U.S. Copyright Law. Requests for permission for extended quotation from or reproduction of this thesis in whole or in parts may be granted only by the copyright holder.

Scott N. Montross
April 2007

ACKNOWLEDGEMENTS

I would like to graciously thank my mentor and graduate advisor, Dr. Mark Skidmore, for his inspiring leadership, generosity, and patience over the past two years. I also thank my committee members, Drs. David Mogk and Gill Geesey for their insightful comments and discussions throughout the development and execution of all experiments included in this thesis. Thank you to Dr. Xner for keeping it real, from the frigid Poles to the steamy bayou of Louisiana, and to Martyn Tranter for his illuminating conversations on subjects from glaciology to mountain biking. I would also like to thank Galena Ackerman who is the best friend, colleague, and partner anyone could ever have. To my family, thank you for listening to me ramble about this on the phone, sorry there will be more. I also thank the Microbial Life Educational Resources at SERC and David Mogk for funding for the first year of my Master's, and to Mark Skidmore for financial support of my field work and funding for the remainder of my studies.

TABLE OF CONTENTS

TABLE OF CONTENTS –CONTINUED

Page

TABLE OF CONTENTS –CONTINUED

Page

LIST OF TABLES

Table Page

LIST OF FIGURES

Figure Page

LIST OF FIGURES-CONTINUED

Figure Page

ABSTRACT

Interactions between dilute meltwater and fine-grained, freshly comminuted debris at the bed of temperate glaciers liberate significant solute. The proportions of solute produced in the subglacial environment via biotic and abiotic processes remains unknown, however, this work suggests the biotic contribution is substantial. Laboratory analyses of microbiological and geochemical properties of sediment and meltwater from the Haut Glacier d'Arolla (HGA) indicates that a metabolically active microbial community exists in water-saturated sediments at the ice-bedrock interface. Basal sediment slurries and meltwater were incubated in the laboratory for 100 days under near in situ subglacial conditions. Relative proportions of solute produced via abiotic v. biotic mineral weathering were analyzed by comparing the evolved aqueous chemistry of biologically active (live) sediment slurries with sterilized controls. Aqueous chemical analyses indicate an increase in solute produced from mineral weathering coupled with nitrate depletion in the biologically active slurries compared with the killed controls. These results infer that microbial activity at HGA is likely an important contributor to chemical weathering associated solute fluxes from the glaciated catchment. Due to the magnitude of past glaciations throughout geologic time (e.g., Neoproterozoic and Late-Pleistocene), and evidence that subglacial microbial activity impacts mineral weathering, greater consideration needs to be given to cold temperature biogeochemical weathering and its impact on global geochemical cycles.

CHAPTER 1

INTRODUCTION

Subglacial Biogeochemistry

Studies in a variety of glacial environments have demonstrated that active and viable microbes can be found in glacier runoff and basal ice (Sharp et al., 1999; Skidmore et al., 2000; Foght et al., 2004) and in sediments in proglacial forefields (Gounot 2001; Sigler and Zeyer 2002). Variations in the concentration of nitrate (NO_3^-) in subglacial meltwaters suggests that microbial processes (e.g., denitrification) may have a significant impact on the chemistry of meltwater draining from the subglacial system (Tranter et al., 1993; Tranter et al., 1997). Studies on melted basal ice incubated at near freezing temperatures indicates that bacteria are metabolically active at 0.3°C (Skidmore et al., 2000) and there is strong evidence that microbial activity at near freezing temperatures influences the chemical weathering of sediments at the glacier bed (Sharp et al., 1999; Tranter et al., 2002; Bottrell and Tranter, 2002; Skidmore et al., 2005; Tranter et al., 2005).

Fine grained sediments at the bed of temperate-based ice masses provide favorable conditions for bacterial activity, since a) the sediments are water-saturated since liquid water is present from basal melting and the delivery of surface meltwater to the glacier bed, b) sediments consist of freshly comminuted chemically reactive debris that is susceptible to colonization by bacterial cells, and c) basal water is at a constant temperature (~ 0-1^{o}C) since the overlying ice insulates the bed from annual surface

temperature fluctuations, and d) contain organic carbon from in-washed organic material from the glacier surface, or from the overriding of preglacial sediments and soils by the ice mass (Skidmore et al., 2000). Together these factors facilitate biogeochemical processes in the subglacial environment as shown in Figure 1.1.

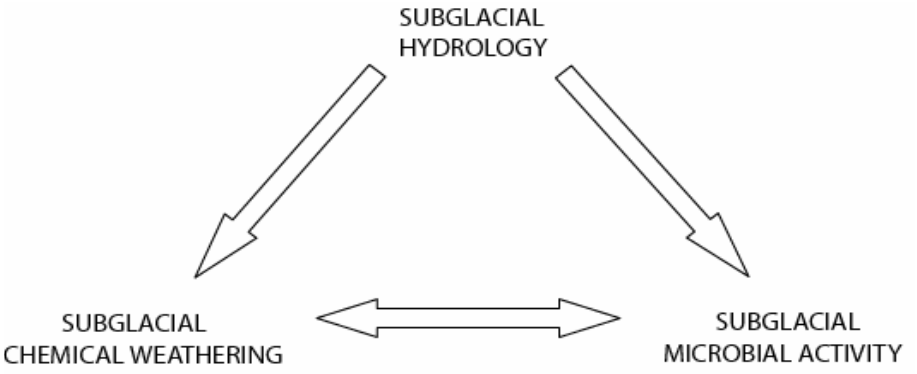

Figure 1.1. Physical, Chemical, and Biological Interactions in the Subglacial Environment. Liquid water, nutrients, and dissolved oxygen are necessary components of subglacial biogeochemical reactions. Therefore subglacial hydrology has a first order control on subglacial chemical weathering and microbial activity in the subglacial environment (depicted by the single headed arrows). An intrinsic link exists between subglacial chemical weathering reactions and subglacial microbial activity (depicted by the double headed arrow). Abiotic chemical weathering reactions may produce dissolved ions (e.g., Mg^{2+}), which may be available to the microbial community. Subglacial microbial activity may also impact the chemical weathering regime of the subglacial environment via chemical transformations of solid and aqueous phase chemical constituents.

Microbial populations are widespread in the subglacial environment of the temperate-based Haut Glacier d'Arolla (HGA) (Sharp et al., 1999), and there is increasing evidence that points to a significant role for microbes mediating the dissolution and oxidation of minerals in sediments beneath ice masses where liquid water is present (Sharp et al., 1999; Skidmore et al., 2000; Tranter et al., 2002; Tranter et al., 2005). However, it remains unknown, quantitatively, what proportion of solute is

generated in the subglacial environment by biotic vs abiotic processes. HGA was chosen as a study site for this research since there have been more than 40 publications describing the hydrologic (e.g., Hubbard et al., 1995; Harbor et al., 1997; Arnold et al., 1998; Nienow et al., 1998; Mair et al., 2001), geochemical (e.g., Brown et al., 1994, 1996; Tranter et al., 1996, 1997, 2002; Mitchell et al., 2001, 2006), and microbiological (e.g., Sharp et al., 1999) attributes of HGA.

Hypothesis

Microbial activity at near freezing temperatures in the water-saturated sediments at the bed of temperate glaciers (e.g., HGA) mediates the dissolution of minerals and increases the generation of solute (e.g., Ca^{2+}, Mg^{2+}, Na^{+}, K^{+}, HCO_3^{-}, and SO_4^{2-}) into subglacial meltwater.

Project Objectives

The main objective of this research was to determine the relative contributions of biotic and abiotic processes to mineral weathering in subglacial sediments. Specific objectives are as follows:-

Objective 1. Determine the chemical composition, bacterial cell biomass and composition of the microbial community using 16S rRNA gene sequences of subglacial meltwater and sediment from HGA.

Objective 2. Measure the changes in the aqueous chemistry from water:sediment mixtures from the subglacial environment at HGA under simulated in situ

conditions, dark and cold (~2^{o}C) for 100 days with a) the indigenous bacteria present and b) in parallel abiotic (killed) controls. Both oxic and anoxic conditions were investigated.

There is an intimate relationship between subglacial hydrology, subglacial chemical weathering environments, and subglacial microbial activity (Tranter et al., 2005). These parameters are dependent on the thermal regime of the glacier and the configuration of the subglacial drainage system. A brief review of these topics follows.

Thermal Regime of Glaciers

The temperature of the ice is an important factor in the characterization of a glacier system since the rates of erosion, deposition, and meltwater production are governed by the thermal regime. Ice masses may be classified into three categories based on the temperature regime of the ice; (a) cold, (b) polythermal, and (c) temperate (Paterson, 1994). Cold-based ice masses consist of ice with temperatures below freezing throughout and liquid water is only present in the veins between ice crystals, with no significant water layer at the glacier bed. Sections of the bed of polythermal ice masses are frozen to the bed especially beneath the thinner margins and termini, however the bed is temperate beneath the thicker, inner zones of the ice mass. Where the bed is temperate, melting occurs and there is a layer of liquid water. Water from the glacier surface can also reach the bed in polythermal ice masses via moulins and crevasses (Skidmore and Sharp, 1999). Temperate-based ice masses, have ice at the bed which is at the pressure-melting point throughout, and thus the entire glacier bed is wet based (Benn and Evans,

1998). The surface of the ice remains snow covered during the winter, and during the summer ablation season surface meltwater is delivered to the glacier bed via crevasses and moulins from surface snow and ice melt. Valley glaciers in mid-latitudes such at HGA are temperate and exhibit year round wet-based conditions across the entire glacier bed (Nienow et al., 1998).

Hydrology of Temperate-based Ice Masses

Waters derived from surface and internal melting processes are delivered to the bed of temperate glaciers via moulins and englacial channels. Surface inputs usually reach a peak in late summer, whereas inputs from basal melting remain relatively stable and exist over the entire year (Nienow et al., 1998). Glacier meltwaters can be divided into three types based on the pathway of the waters to the glacier terminus; these are supraglacial, englacial, and subglacial meltwaters. Water flowing from the subglacial stream(s) at the terminus of temperate based glacier systems (e.g., HGA) is a composite of these three types of meltwaters (Tranter et al., 2002). Supraglacial meltwaters flow in streams on the glacier surface and are derived primarily from the melting of snow and ice and are dilute (EC < 10 $\mu S\ cm^{-1}$) (Sharp 1988; Sharp et al., 1999). Englacial meltwaters are also dilute, and essentially debris free waters produced from icemelt and are routed through the glacier and eventually to the bed (Fountain and Walder, 1998; Fountain et al., 2005). Subglacial meltwaters are waters that are routed at the bed, and these waters have elevated sediment and solute loads since they are in contact with basal sediments (Fountain and Walder, 1998).

The flowpaths of water to the glacier bed and the seasonal evolution of the subglacial drainage system of a temperate-based glacier are shown in Figure 1.2. Two types of subglacial drainage configuration exist beneath temperate-based glaciers; channelized drainage systems (quick flow) and distributed drainage systems (delayed flow) (Fountain and Walder, 1998). The distributed systems include water derived from snowmelt that percolates slowly to the glacier bed, thin layers of water from basal melting, and water saturated till between the bedrock and the overlying ice. These zones are hydraulically inefficient due to the low porosity of the till. Sediment:water interactions are high in the distributed drainage system due to the slow water flow rates (<0.05 m sec^{-1}), compared to flow rates in the channelized drainage system (0.5 m sec^{-1}) (Nienow et al., 1998).

The surface of the glacier is snow covered, during the winter months and water movement is limited to the intergranular percolation of pore water through the snowpack and glacier ice, to the distributed drainage systems at the glacier bed (Figure 1.2a). The morphology of the subglacial drainage system changes over the course of the melt season (Figure 1.2b). Nienow et al. (1998) demonstrated that a system of major channels develops at the glacier bed at HGA as the melt season progresses at the expense of a hydraulically inefficient distributed system. Headward growth up-glacier of the channelized subglacial system follows the retreating snowline since a change in surficial characteristics from snow to ice results an increase in the volume of runoff (due to lower albedo) into moulins and crevasses and ultimately the glacier bed (Figure 1.2b,c).

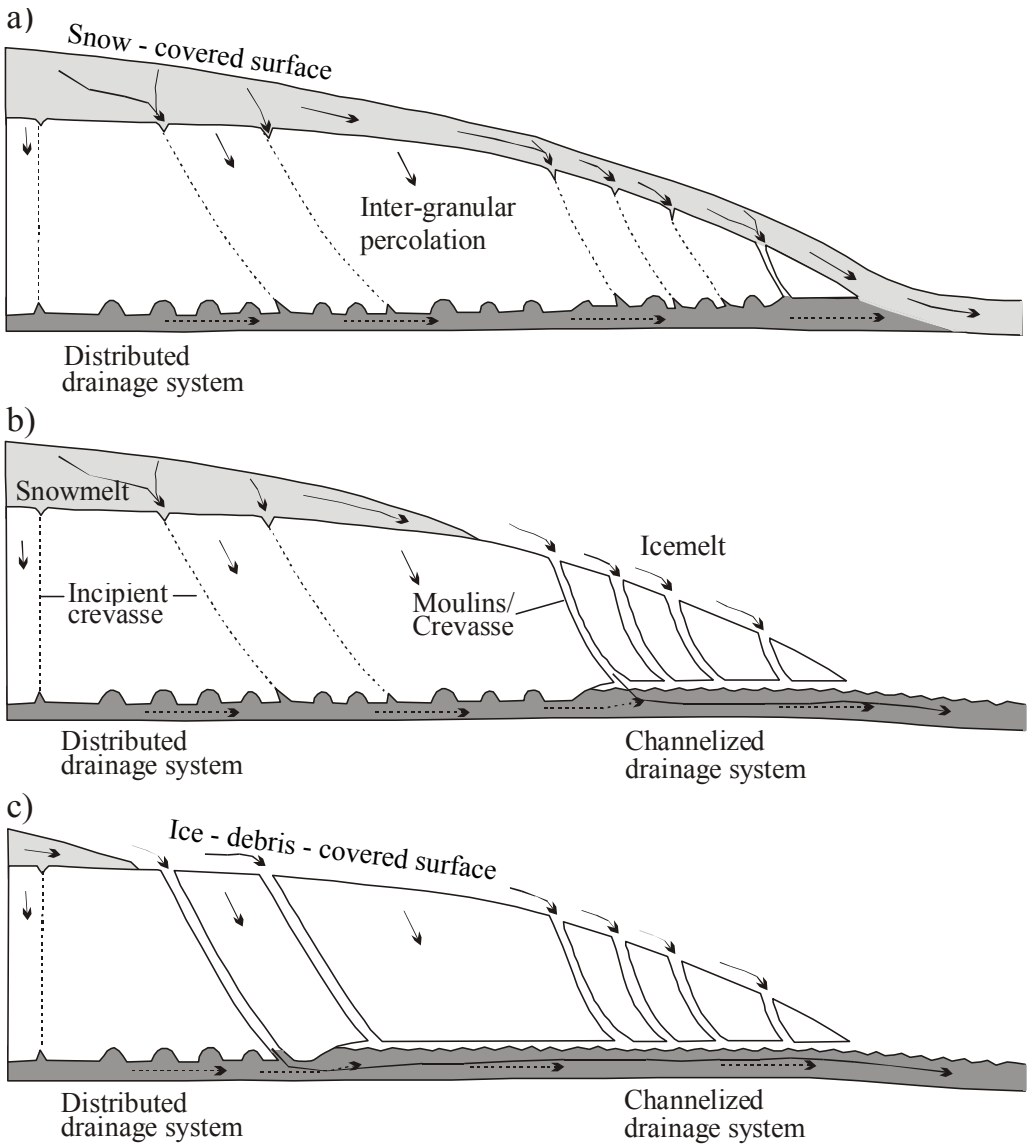

Figure 1.2. Seasonal development of the subglacial drainage system of a temperate-based glacier (modified from Kivimäki, 2005). Winter configuration (a), mid-melt season (b), late-melt season (c).

The delivery of supraglacial water into the subglacial drainage system induces high water pressures within the distributed drainage system, which causes it to evolve rapidly into a channelized system (Nienow et al., 1998). Kamb et al. (1987) suggested distributed cavity systems collapse into channelized systems when they are subjected to water pressure perturbations above the steady state value. These perturbations are the result of a switch from steady state laminar sheet flow to a high pressure turbulent flow which eventually increases the cross-sectional area of the conduit. The subglacial drainage system is dominated by channelized drainage during the summer months. However, the basal sediment layer that flanks the margins of the channelized system that is referred to as the channel marginal zone (CMZ) is a favorable environment for biogeochemical reactions (Hubbard et al., 1995). The CMZ is composed of reactive fine grained sediments and during times of high discharge water from the channelized drainage system floods the sediments lining the conduit walls. Since all zones of the channelized drainage and are likely oxic to sub-oxic (Tranter et al., 2005), the CMZ may be a key site for biogeochemical reactions in the presence of oxygen between bacteria and subglacial debris.

Subglacial Chemical Weathering at HGA

This section on will focus on previous work on subglacial chemical weathering processes at HGA (Tranter et al., 1993, 1997, 2002). Carbonation reactions and the coupled reactions of sulfide oxidation and carbonate dissolution are believed to be the dominant chemical reactions occurring in the subglacial environment of HGA (Tranter et al., 1993) and other alpine glaciers (Anderson et al., 1997; Hosein et al., 2003; Skidmore

et al., 2005). The carbonation of silicates (Equation 1.1) and carbonates (Equation 1.2) are rapid reactions and are believed to occur in the major subglacial arterial channels (i.e., channelized drainage system). These reactions involve H^+, from the dissociation of carbonic acid, as a proton source (Tranter et al., 2002). However, carbonation is not necessarily confined to the major arterial channels in the subglacial environment and can also occur in the CMZ and distributed system since other subglacial CO_2 sources may exist, e.g. via the oxidation of organic carbon (Tranter et al., 2005).

Equation 1.1 Carbonation of feldspar (anorthite) surfaces

$$CaAl_2Si_2O_{8(s)} + 2CO_{2\,(aq)} + 2H_2O_{\,(l)} \rightarrow Ca^{2+}_{(aq)} + 2HCO_3^-{}_{(aq)} + H_2Al_2Si_2O_{8(s)}$$

Equation 1.2 Carbonation of carbonate

$$CaCO_{3\,(s)} + CO_{2\,(aq)} + H_2O_{\,(l)} \rightarrow Ca^{2+}{}_{(aq)} + 2HCO_3^-{}_{(aq)}$$

The dominant chemical weathering reactions in the distributed (slow) drainage system are believed to be sulfide oxidation coupled with carbonate dissolution (Equation 1.3). In the distributed drainage system the rate of sulfide oxidation is controlled by the pH of the water, temperature, concentrations of Fe^{2+} and Fe^{3+}, and most importantly the dissolved oxygen concentration of the water (Tranter et al., 2002 and references within).

Equation 1.3 Sulfide oxidation coupled to carbonate dissolution

$$4FeS_{2(s)} + 16Ca_{1-x}(Mg_x)CO_{3(s)} + 15O_{2(aq)} + 14H_2O_{(l)} \rightarrow$$

$$16(1-x)Ca^{2+}_{(aq)} + 16xMg^{2+}_{(aq)} + 16HCO_3^-{}_{(aq)} + 8SO_4^{2-}{}_{(aq)} + 4Fe(OH)_{3(s)}$$

Subglacial Microbial Activity at HGA

Variations in the concentration of nitrate (NO_3^-) in subglacial meltwaters at HGA suggests that microbial processes (e.g., denitrification) may have a significant impact on the chemistry of meltwater draining from the subglacial system (Tranter et al., 1993; Tranter et al., 1997). Some borehole waters from HGA are characterized by a high concentration of SO_4^{2-} and anoxic conditions (Tranter et al., 2002). $\delta^{18}O$ of SO_4^{2-} in runoff from HGA also show compelling evidence for suboxic conditions (Bottrell and Tranter, 2002). Chemical and isotopic measurements infer that an additional source of oxygen is present in the subglacial environment since the high SO_4^{2-} levels found (up to 1200 μeq L^{-1}) are greater than could be achieved if sulfides are oxidized by dissolved oxygen in saturated water at 0°C (c. 414 μeq L^{-1}) (Tranter et al., 2002). Subglacial meltwater chemistry from HGA indicates that pyrite (FeS_2) oxidation proceeds past oxygen depletion, continuing under anoxic conditions using Fe^{III} present in silicate minerals to produce further sulfate (Tranter et al., 2002). Previous work by Sharp et al. (1999) on the geomicrobiology of the subglacial environment of HGA provided a measurement of bacterial biomass in meltwater but did not address whether or not these cells were viable or metabolically active.

Subglacial Geomicrobiology

Significant investigations into the geomicrobiology of glacierized basins have identified bacterial populations under temperate valley glaciers (Sharp et al., 1999; Foght

et al., 2004; Skidmore et al., 2005), an Arctic polythermal glacier (Skidmore et al., 2000), and sub-glacial lakes (Karl et al., 1999; Priscu et al., 1999; Christner et al., 2001; Gaidos et al., 2004) and there is evidence that microorganisms may be important contributors to subglacial geochemical weathering (Sharp et al., 1999; Skidmore et al., 2000; Wadham et al., 2004). There is increasing evidence that points to a significant role for microbes mediating dissolution and oxidation of minerals in sediments where liquid water is present in the subglacial environment (Sharp et al., 1999; Skidmore et al., 2000; Tranter et al., 2002; Foght et al., 2004; Skidmore et al., 2005; Tranter et al., 2005). Thus it is likely that where temperate basal conditions exist under valley glaciers and contemporary ice sheets microbial activity has an impact on the generation of solute in the subglacial environment.

Low Temperature Weathering Experiments

Laboratory controlled weathering experiments are a practical method to simulate subglacial geomicrobiological weathering (Sharp et al., 1999) since access to the subglacial environment is limited. Previous work to simulate subglacial geomicrobiological weathering has been performed with debris-rich ice collected from the margins of the Glacier d'Tsanfleuron, Switzerland (Sharp et al., 1999). Sharp et al. (1999) demonstrated that microbially catalyzed rates of sulfide (e.g., FeS_2) oxidation are likely two orders of magnitude greater than abiotic reaction rates, calculated from theoretical values (Nicholson et al., 1988). These results indicate microbial activity is likely to be the dominant influence on the rate of sulfide oxidation and sulfate production in the subglacial environment (Sharp et al., 1999; Tranter et al., 2002). Although the

experiments by Sharp et al. (1999) demonstrated a high rate of FeS_2 oxidation when bacteria were present, their experiments did not include a killed/abiotic control. Therefore the relative rates of microbially-mediated (biotic) vs. the rates of inorganic (abiotic) sulfide oxidation could not be determined. Experiments by Kivimäki (2005) were conducted using crushed proglacial sediment and meltwater, and these experiments included a series of killed controls but these experiments were conducted only under oxic conditions. Kivimäki (2005) showed that microbial activity under oxic conditions resulted in the release of Ca^{2+}, Mg^{2+}, Na^{+}, and K^{+} over a 300 day incubation at ~2°C.

The experiments conducted for this thesis contrast the previous work at HGA by Sharp et al. (1999) in that greater consideration was given to the design of the experiment in order to mimic *in situ* subglacial conditions- e.g., cold, dark, oxic and anoxic. Sediments and meltwater used in this experiment were collected from the meltwater stream exiting the terminus of HGA at the end of the summer meltseason. The meltwater and sediment collected for this experiment are a good representative sample of the subglacial environment for the following reasons. Meltwaters collected in the late season are dominated by subglacially derived water since surface inputs have ceased due to freezing temperatures at the glacier surface in mid-October (beginning of winter in Swiss Alps). Sediments collected from shallow pools in the subglacial stream in the meltwater tunnel at the terminus are assumed to have been recently deposited via meltwater flushed from the glacier during the meltseason. Water: sediment ratios for this experiment were selected to ensure that sufficient mixing and flushing of sediment pore spaces was possible and to ensure sufficient volumes of sample could be collected for all desired analyses. Sediment: water incubations were conducted under oxic and anoxic conditions

since the subglacial environment is likely comprised of zones which are oxic or anoxic (Bottrell and Tranter, 2002).

Broader Implications

Mineral Weathering in Glacierized Basins

Studies of the chemistry of meltwaters from various glacierized catchments show that subglacial meltwaters are elevated in dissolved Ca^{2+}, K^{+}, HCO_3^{-}, and SO_4^{2-} relative to non-glacial run-off (Sharp et al., 1999; Anderson et al., 1997, 2000). In general silica dissolution rates are lower in glacierized catchments than in non-glaciated catchments with the same discharge (Anderson et al., 1997) since silica dissolution rates in the subglacial environment are most likely retarded due to the temperature dependent nature of silicate weathering (White et al., 1999a; Anderson et al., 2000). In glaciated catchments silicate weathering inhibition is imposed by low temperatures and a lack of established vegetation (Anderson et al., 1997). Anderson et al., (2000) showed that silica dissolution rates increased in the glacier foreland when vegetative cover was present, but the rate did not exceed the rate of silica dissolution in non-glaciated catchments.

It is widely accepted that calcite dissolution is a dominant weathering reaction in the subglacial environment (Tranter et al., 1994, 1997, 2005). At neutral pH, the calcite dissolution rate is approximately 11 orders of magnitude faster than the dissolution rate of albite (Hosein et al., 2003). Calcite may be an accessory mineral in crystalline rocks and is not confined to catchments dominated by carbonate geology (White et al., 1998). White et al. (1999b) observed that calcite provides up to 98% of the calcium flux from powdered granitic rocks in laboratory dissolution experiments, and it appears that glacial

weathering processes may optimize the dissolution of calcite within glaciated catchments underlain by crystalline bedrock (Hosein et al., 2003) and it is plausible that microbes increase calcite dissolution rates relative to abiotic processes.

Global Biogeochemical Cycles

Calculations of terrestrial weathering and erosion rates by Gibbs and Kump, (1994) assume significant chemical erosion does not occur beneath ice sheets. Therefore the contribution of subglacial biogeochemical weathering to chemical weathering fluxes is assumed to be zero. Yet it is likely this contribution is greater than zero due to the combinations of high physical and chemical denudation rates (Anderson et al., 1997) and the presence of metabolically active bacteria in the subglacial environment (Skidmore et al., 2000). Due to the extent of pervasive glaciations over geologic time (e.g., Neoproterozoic and Late-Pleistocene) and current ice cover (c. 10% of the Earth) further consideration should be given to cold-temperature biogeochemical weathering and its impacts on global biogeochemical cycles. Furthermore, widespread deglaciation (Houghton et al., 2001) has resulted in the exposure of reactive, bacterial laden subglacial sediments from beneath the overlying ice mass. Exposure of these sediments and their associated microbiota to oxygenated conditions at the Earth's surface has further implications to weathering and solute generation from the proglacial forefields of the retreating glaciers.

CHAPTER 2

FIELD SAMPLING AND ANALYSIS OF FIELD SAMPLES

Description of Study Site

The Haut Glacier d' Arolla (HGA) is a temperate alpine glacier located at the head of the western branch of Val de Herens, Valais, Switzerland (see Figure 2.1). Approximately 54% of the 11.7 km^2 catchment area is glacierized and the glacier is c. 4 km long (Sharp et al., 1995; Bottrell and Tranter, 2002). It is important to note that these measurements were made in 1993 and are an overestimate of the current ice volume due to retreat of the glacier. The location and elevation of the glacier terminus and sampling sites was measured in October 2004 by GPS (Garmin® International, U.K.) at 45º58'N 7º32'E and 2538 m a.s.l. respectively. HGA is underlain by igneous and metamorphic rocks of the Arolla series of the Dente Blanche Nappe and is comprised mainly of gneisses, hornblende–biotite–tonalites, hornblende–biotite–quartz diorites and gabbros (see Figure 2.1), and these units contain trace amounts of geochemically reactive trace minerals, e.g., calcite and pyrite (Tranter et al., 1997).

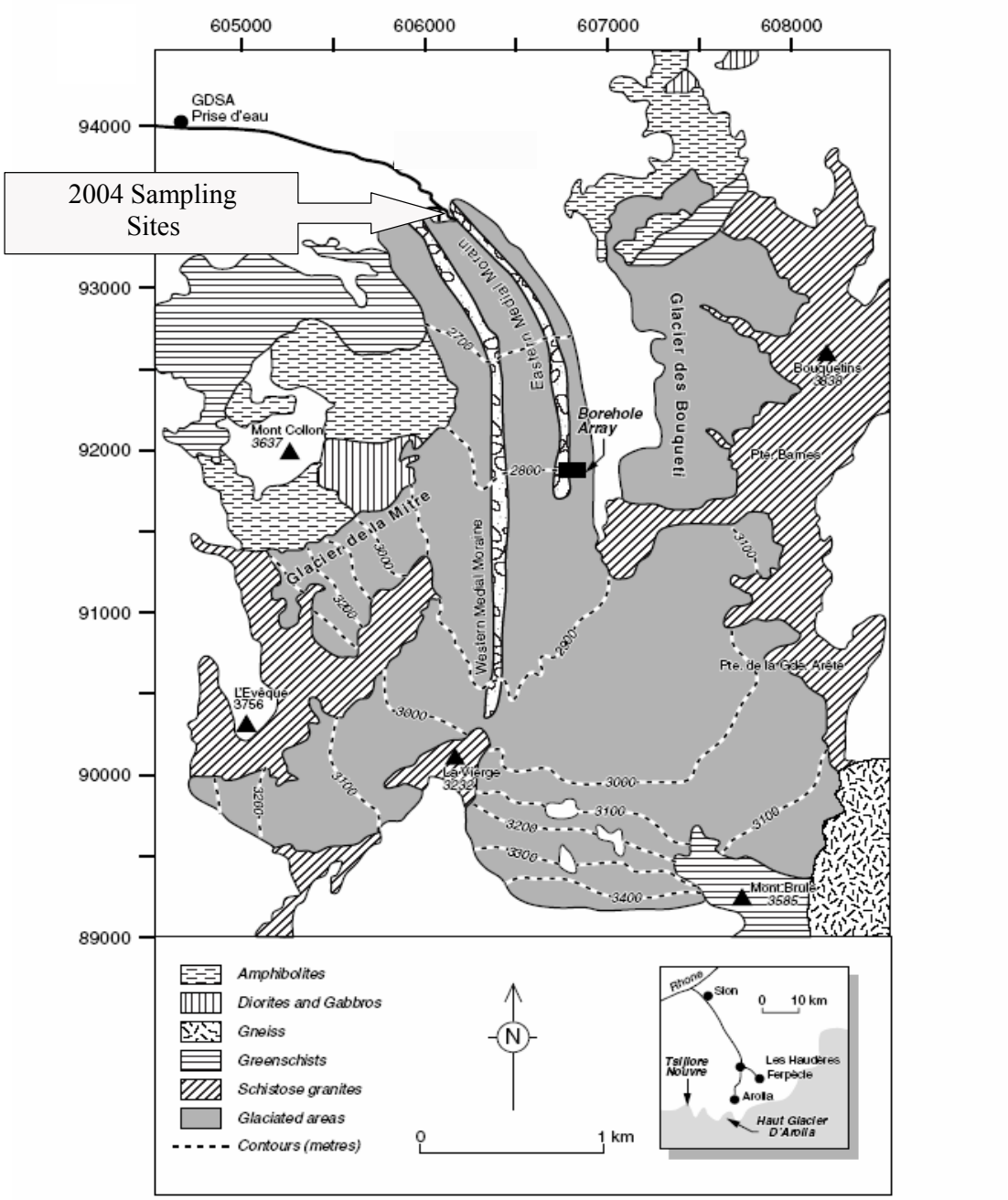

Figure 2.1. Location Map of Haut Glacier d'Arolla, Valais Switzerland. Highlighted on this map are sampling sites, elevation of glacier surface (m a.s.l.), and geology of the study area. This map was modified from Tranter et al. (2002).

Subglacial Chemistry and Microbiology

Waters and sediments (see Table 2.1) were collected from the left and right subglacial streams at the terminus of HGA (see Figure 2.2). Electrical conductivity (EC) and pH of HGA stream water was measured using an Accumet EC meter and Orion 290A pH meter respectively.

Table 2.1. Sample matrix for field samples collected from HGA. Volumes listed are the amounts collected from each stream.

Material	Sample Volume (cc)	Intended Analysis
meltwater	45	pH
meltwater	45	DOC
meltwater	1000	ion analysis
meltwater	250	cell counts
meltwater	4000	DNA extraction
meltwater	12000	sediment dissolution experiment
sediment	1000	cell counts and molecular biology
sediment	12000	sediment dissolution experiment

Water samples for dissolved organic carbon (DOC) were immediately filtered in the field through a nylon 0.1 μm filter (Fisherbrand cat. no. 09-719C) into a pre-combusted (550°C) EPA vial. Water samples for microbial enumeration were collected into a pre-combusted (550°C) 250 mL glass bottles containing 0.2 μm filter sterilized formaldehyde (final concentration 3.7% w/w). Water samples for ion chemistry were collected following a 3x rinse with stream water in an acid-washed 1 L Nalgene bottle and water for samples for DNA were collected following a 3x rinse with stream water in a sterile Nalgene bottle.

Figure 2.2. Terminus of Haut Glacier d' Arolla (a). In October 2004 sediments and meltwater were collected from the two (subglacial streams (b and c).

The samples were transported back to the field laboratory at near-zero temperatures. 1000 mL of stream water was filtered through a 0.4 μm filter (Millipore cat. no. 109817-1) for ion chemistry using a Nalgene filter system and hand pump. Aliquots of the filtrate were poured into 20 mL HDPE scintillation vials, following a 3x rinse with the filtrate. All samples were filtered in the field < 5 hours after collection. Water samples for DOC, anion and cation analysis and cell counts were stored at 4^{o}C in the field laboratory and kept on ice for transport back to Montana State University (MSU), and stored at 4°C until analysis.

Bacterial cells in HGA meltwater were collected by filtering 1000 mL of stream water onto 47 mm diameter pre-sterilized 0.22 μm Millipore GS filters using a Nalgene filtration apparatus and hand pump. The filter apparatus was re-sterilized between samples as follows; a blue non-permeable filter membrane spacer (Millipore type GS) was inserted onto the filter platform, and the upper chamber of the filter device was sealed to the filter base. The upper (input) chamber was rinsed 3x with 3% hydrogen peroxide, 1x with 5% Nitric acid solution, followed by 3x rinse with sterile Nanopure water. The filter paper was added, then the filter apparatus was then rinsed 3x with sample prior to the filtration. Procedural blanks were prepared by filtering 1000 mL of sterile Nanopure water through the same apparatus in the field. All filters were placed in MO BIO^{TM} bead beat tubes, frozen in the field and transported back to the laboratory frozen and stored at -80°C until processing.

Water and Sediment Sampling for Weathering Experiments

Subglacial meltwater and sediment for use in the laboratory dissolution experiment were collected from the left and right subglacial streams at the terminus of HGA (Table 2.1). Water was collected by grab sample into autoclave sterilized 4 L Nalgene bottles that were pre-rinsed 3x with stream water before collecting the final sample. Sediments were collected from pools on the margins of the meltwater stream using alcohol (70%) flame sterilized tools and stored in autoclave sterilized Nalgene bottles. Water and sediment samples collected for laboratory weathering experiments were frozen at -20°C in the field laboratory and shipped frozen to the laboratory at MSU.

Water Chemistry Analysis

Major ions in water samples were determined with a Metrohm-Peak ion chromatograph using protocols developed from the manufacturer's instructions. The eluent flow rate was 0.7 mL min^{-1} for anions and 1.0 mL min^{-1} for cations, and the sample loop was approximately 250 µL for all samples and standards. The concentration of major cations, sodium (Na^+), calcium (Ca^{2+}), magnesium (Mg^{2+}), ammonium (NH_4^+), and potassium (K^+) were measured using a Metrosep C-2-250 analytical column (4 x 250 mm). The eluent was a 4 mmol L^{-1} tartaric acid/ 0.75 mmol L^{-1} dipicolinic acid solution. Fluoride (F^-), chloride (Cl^-), nitrate (NO_3^-), phosphate (PO_4^{3-}), sulfate (SO_4^{2-}), organic acids of formate ($CHOO^-$), and acetate (CH_3COO^-) were measured using a Metrosep A-2-250 (4 x 250 mm) analytical column, and chemical suppression with 100 mM H_2SO_4. The eluent was a 3.2 mmol L^{-1} sodium carbonate / 1.0 mmol L^{-1} sodium hydrogen

carbonate solution. The final concentration of each ion was calculated with a linear equation derived from the standard curve of peak area vs. concentration (mV sec^{-1} vs. mg L^{-1}) for each standard (0.1 - 10.0 mg L^{-1}). Precision, calculated as the coefficient of variation, for all major ions was < 3 % for all ions, except for K^+ and PO_4^{3-} where precision approaches 6 % and 10 % respectively. Accuracy, calculated as the relative mean error with respect to known standards (Fluka Inc., cat. nos. 89886 and 89316), ranged from < 1 % to 6 % for all major cations and anions. Laboratory prepared standards, certified standard solutions (Fluka Inc., cat. nos. 89886 and 89316; Hamilton Inc., cat. no. 09821), and blanks were analyzed at the beginning of each run, during the run every eight samples, and at the end for quality assurance and quality control.

Direct Microscopic Counts

Bacterial Cells in Subglacial Meltwater

Samples of meltwater (10 mL) fixed in the field (final concentration of 3.7% formaldehyde v/v) were stained with SYBR Gold ™ (Molecular Probes, Inc., cat. no. S-11494) for 15 minutes in the dark. The sample was then filtered onto a 25 mm diameter-0.2 µm black polycarbonate filter (Poretics, cat. No. K02BP02500) using a filtration manifold and vacuum (25 kPa). Filters were mounted on glass slides with the addition of an antifade solution, which consisted of 0.1% p-phenylenediamine (Sigma cat. no. P-1519) in a 1:1 solution of phosphate-buffered saline (PBS) and glycerol. All filtering and manipulations were conducted within a Labconco ™ class 100 purified air bench, equipped with a germicidal UV-lamp. The reagents used for DNA staining and SYBR

Gold preparation were passed through 0.2 μm filters to remove extraneous particles and cells before use.

Bacterial Cells in Subglacial Sediment

A sub-sample (10 g) of the sediment collected in the field was used for the enumeration of bacterial cells. The removal of cells from sediment surfaces was achieved by washing 10 g of sediment with a 1% w/v sodium pyrophosphate solution in a pre-weighed, pre-combusted (550°C) flask containing 10 g of sterilized 3 mm glass beads (Foght et al., 2004). Flasks containing the sample, glass beads, and the washing solution were swirled at 250 rpm for 20 minutes at 4°C, the supernatant was removed and transferred to a 15 mL Falcon™ tube and allowed to settle. The aqueous sample was stained with SYBR Gold for 15 minutes and filtered onto a 25 mm diameter- 0.2 μm black polycarbonate filter (Poretics, cat. No. K02BP02500) using a filtration manifold and vacuum (25 kPa). The remaining sediment and glass bead mixture was dried at 105°C and the results were used for the calculation of cells per gram of dry sediment.

Enumeration of Cells
Using Epifluorescent Microscopy

Cells on the filters from both the waters and sediments were viewed using a Nikon Optiphot epifluorescent microscope, equipped with a DM510 filter cube (Nikon), at a final magnification of 1000X. The total number of cells in each field of view (one field of view at 1000x= 16,741 μm^2) were counted and for each sample a total of 30 fields were viewed. The average number of cells in each sample was calculated by multiplying the average number of cells in the 30 fields viewed by the total number of

possible fields ($A=\pi(16mm)^2$ or 2.01×10^8 μm^2, since only 16 mm of the 25 mm filter was covered in cells) and the total number of possible fields of view was ~12010. This method was adopted from a similar method by Porter and Feig (1980) and Kirchman et al., (1982). Cell numbers in water samples were reported as the number of cells $mL^{-1}$of meltwater. For sediment samples, water content results were calculated using the wet and dry weights of each sample prepared. The corrections of enumeration data to a dry-weight (cells g^{-1} dry sediment) was based on the method described in Foght et al., (2004). Field blanks consisting of filter sterilized Nanopure water were prepared and treated in the same manner as the water samples collected in the field. Laboratory blanks consisting of sterile Nanopure water (water blanks) or heat sterilized 3 mm diameter silica beads (sediment blanks) substituted for the sample and each blank was prepared and treated in the same manner as the samples. The analysis of the field and laboratory blanks indicated that cellular contamination associated with bottle preparation, sample collection, staining, filtering, and microscopy were < 50 cells mL^{-1} in all water samples and < 5 cells g^{-1} in all sediment samples.

Clone Library Construction and Analysis

Genomic DNA extraction

Genomic DNA was extracted from cells collected on filters using mechanical lysis by bead beating (BIOSPEC Products), and the MO BIO ultra clean Soil DNA Isolation Kit (MO BIO, cat. no. G-3197-50). Genomic DNA was extracted from 1-2 g of the same sediment used for bacterial cell counts, following the manufacture's protocol.

DNA Amplification via
the Polymerase Chain Reaction

Archaea specific (348F/1391R) and Bacteria specific (27F/1492R) oligonucleotide primers (Lane, 1991) were used to amplify 16S rRNA genes from genomic DNA extracted from HGA water and sediment. To optimize and limit the biases associated with the polymerase chain reaction (PCR) a gradient of annealing temperatures (50-65°C) were initially used to determine the optimum temperature for each forward and reverse primer set and all reactions were limited to 30 cycles to avoid non-specific amplification due to decreased activity of the polymerase enzyme (Suzuki and Giovannoni, 1994). The final PCR conditions used were, 3 minutes at 95°C (initial denaturation) followed by 45 seconds of denaturation at 95°C, 30 seconds of annealing at 50°C (27F/1492R) and 52°C (348F/1391R), and 90 seconds of extension at 72°C for 30 cycles followed by 5 minutes of final extension at 72°C in a MJ Research PTC-200 thermalcycler.

Ligation and Cloning of 16S rRNA Genes

PCR products (~1.4 kb) from sediment and water samples from the left meltwater stream were used in the construction of DNA clone libraries. No Archaeal PCR products were produced so only Bacterial PCR products were used for the construction of a clone library. The PCR products were ligated into the plasmid vector pGem T-easy (Promega, cat. no. 1211), and transformed into competent *Escherichia coli* cells (Promega, cat. no. 9FB035). The cell suspension was plated on Luretia Broth (LB)-Amp agar plates containing 100 ug mL^{-1} of ampicillin, 100 uL of 0.1 M IPTG and 20 uL of X-GAL (50 mg mL^{-1}). The plates were incubated overnight at 37^{o}C and individual colonies which

grew white were picked using a sterile toothpick, and grown up overnight in liquid LB – Amp (100 µg mL^{-1}) broth. Clonal DNA was re-amplified using the oligonucleotide primers SP6/T7, and the amplified DNA was digested with the restriction endonucleases *EcoR*1 and *Rsa*I (Invitrogen, Carlsbad, CA.). The restriction fragments were resolved on a 2.5% Sodium Borate-agarose gel (SB) (Brody and Kern, 2004) and stained in TAE (20 mmol L^{-1} Tris, 10 mmol L^{-1} acetate, 0.5 mmol L^{-1} EDTA, pH 7.4) containing ethidium bromide (100 µl mL^{-1}) for 20 minutes. Banding patterns for each clone were analyzed using KODAK gel compare software, and grouped into operational taxonomic units (OTU's) by restriction length fragment polymorphism (RFLP). Clones (meltwater n=100 and sediment n=85) displaying unique RFLP patterns were bi-directionally sequenced using primers that annealed to regions flanking T7 and SP6 universal promoter sequences. Sequences were determined on an ABI 2600 (Applied Biosystems) sequencer at the Translational Genomics Institute (TGEN, Phoenix, Az.) and on an ABI 3130 Genetic Analyzer (Applied Biosystems) at McMurdo Station, Antarctica. The sequence data was compiled using Bio-Edit Sequence Alignment Editor (BioEdit, Inc.) to assemble and edit the final consensus nucleotide sequence. The compiled partial 16S rRNA gene sequences were compared to sequences within GenBank using Ribosomal Database Project (RDP-II; Michigan State University, East Lansing) and the basic local alignment search tool (BLAST).

Denaturing Gradient Gel Electrophoresis

Genomic DNA from HGA sediment and water samples from the left and right streams was amplified with PCR/DGGE primers 1070F and 1391GC (Muyzer et al.,

1993). The products were loaded onto a 160 x 160 x 1 mm - 8% polyacrylamide gel in 1x TAE (20 mmol L^{-1} Tris, 10 mmol L^{-1} acetate, 0.5 mmol L^{-1} EDTA, pH 7.4). The polyacrylamide gel was made with a denaturing gradient ranging from 40% to 60% (where 100% denaturant contains 7 M urea and 40% formamide) and poured using a Model 475 Gradient Former (Bio-Rad). The electrophoresis was run for 700 min at 60 V in 1X TAE buffer at a constant temperature of 60°C. The gel plate was cooled in ice water for 5 min and then stained for 20 min in 200 mL of 1x TAE buffer containing 10x SYBR green. The bands were visualized and images of the gels were taken on a Kodak Image Station (Model 200R).

Characterization of Viable Heterotrophic Bacteria

The heterotrophic growth media R2A with agar (Atlas 2005) was inoculated with 100 and 400 µL of water from melted sediment samples collected from the left and right stream, and incubated at 4 and 24°C. Ten colonies which displayed different morphologies were selected and isolated by triple-pass repeat transfers at 4 and 24°C. Isolates which grew at 4°C were characterized by colony morphology, cell morphology (gram stain and phase contrast microscopy) and 16S rRNA gene sequence. Genomic DNA was extracted from the ten isolates and bacterial 16S rRNA genes were amplified by PCR using the oligonucleotide primers 27F/1492R. The amplified DNA was digested with the restriction endonuclease *EcoR*I (Invitrogen, Carlsbad, CA.), and the restriction fragments were resolved on a 2.5% Sodium borate agarose gel. 16S rRNA genes from isolates with a unique RFLP pattern were sequenced and compared to known sequences using the BLAST search tool (Altschul et al., 1990).

CHAPTER 3

RESULTS

Subglacial Meltwater Chemistry

Field Samples

Electrical conductivity (EC) a measurement of the presence of dissolved solids (e.g., ions in solution) in meltwater from subglacial streams at HGA ranged from 55.1-61.3 μS cm^{-1} (Table 3.1). Table 3.1 shows the pH, EC, dissolved organic carbon (DOC), and the measured concentration of sodium (Na^+), potassium (K^+), calcium (Ca^{2+}), magnesium (Mg^{2+}), fluoride (F^-), chloride (Cl^-), nitrate (NO_3^-), phosphate (PO_4^{3-}), sulfate (SO_4^{2-}), and $*HCO_3^-$ ions in water from the two streams studied. Subglacial meltwater draining from the left and right portals are generally comparable with respect to pH, conductivity, and the concentration of major cations and anions. The dominant cation in both streams was Ca^{2+}, followed by Mg^{2+}, Na^+, and K^+ in order of decreasing concentration. The dominant anion in both streams was $*HCO_3^-$ (* calculated using PHREEQci, Parkhurst, 1995), followed by SO_4^{2-}, NO_3^-, F^-, and Cl^- in order of decreasing concentration. The solute compositions of late season meltwaters from HGA are dominated by Ca^{2+}, Mg^{2+}, and HCO_3^- and SO_4^{2-}. The Ca^{2+}/SO_4^{2-} ratio and the sulfate mass fraction (S-ratio) $[SO_4^{2-}/ (SO_4^{2-} + HCO_3^-)]$ are indicators of the dominant solute producing weathering processes and can be used to identify sulfide oxidation and calcium dissolution as major weathering processes (Tranter et al., 2002).

Table 3.1. Subglacial stream chemistry data for HGA.

Chemical Parameter	Stream Left	Stream Right
pH	7.8	8.3
Electrical conductivity	61.3	55.1
Na^+	24.0	18.4
K^+	17.6	16.3
Ca^{2+}	1135.7	1035.0
Mg^{2+}	86.6	52.1
F^-	8.2	7.2
Cl^-	2.4	2.4
NO_3^-	21.4	20.2
PO_4^{3-}	0.1	0.2
SO_4^{2-}	409.0	335.0
$*HCO_3^-$	814.8	741.5
Organic carbon	0.2	0.2

* Calculated by charge deficit using PHREEQci software (Parkhurst, 1995)

Units are μeq L^{-1} except pH, EC (μS cm^{-1}), and organic carbon (mg L^{-1})

The stoichiometry for pyrite oxidation coupled to carbonate dissolution (Equation 3.1.) produces a Ca/SO_4 ratio of 2 and an S-ratio of 0.5 for concentrations in μeq L^{-1}. Assuming that other sources of sulfate are small, the S-ratio provides a crude index of HCO_3^- derived from linked sulfide oxidation and carbonate dissolution (SO-CD) relative to other sources of HCO_3^- (Tranter et al., 2002).

Equation 3.1. Pyrite oxidation coupled to carbonate dissolution

$$4FeS_{2(s)} + 16CaCO_{3(s)} + 15O_{2(aq)} + 14H_2O_{(l)} \rightarrow$$

$$16Ca^{2+}_{(aq)} + 16HCO_3^-{}_{(aq)} + 8SO_4^{2-}{}_{(aq)} + 4Fe(OH)_{3(s)}$$

The S-ratio of waters dominated by sulfide oxidation and carbonate dissolution reactions should be c. 0.5. Carbonation of carbonates drives this value to < 0.5, while sulfide oxidation coupled with silicate dissolution drives this value to > 0.5 (Tranter et al., 2002). The calculated Ca^{2+}/SO_4^{2-} ratio and S-ratio for subglacial stream water analyzed for this study is shown in Table 3.2. The Ca^{2+}/SO_4^{2-} ratio and S-ratio in water from both streams were similar, c. 3.0 and 0.3 respectively. The excess of Ca^{2+} over SO_4^{2-} in the waters indicates these solutes are derived primarily from carbonate dissolution reactions, and S-ratios of 0.3 indicate carbonation of carbonates (Tranter et al., 2002). However, sulfide oxidation likely produces 300- 400 μeq L^{-1} of sulfate in the subglacial meltwater and an equivalent amount of carbonate dissolution likely occurs via SO-CD (Equation 3.1).

Table 3.2. Subglacial stream water Ca^{2+}/SO_4^{2-} and S ratios for HGA.

	Ratio	
	Ca/SO_4	S
Left stream	2.8	0.3
Right stream	3.1	0.3

Meltwater with an S-ratio of 0.3 is considered to be representative of subglacial water flowing in more efficient parts of the distributed drainage system at HGA (Tranter et al., 2002). The similarity in chemistry (i.e, concentrations of major ions, Ca^{2+}/SO_4^{2-} ratio, and S-ratio) between the two streams flowing from the terminus of HGA likely results from; a) similar inputs of waters via precipitation and icemelt which is delivered to the glacier bed during the melt season, and (b) similar hydrologic flow paths resulting in similar water residence time and water/sediment ratios.

Solute Provenance in Stream Waters

Balance Between Atmospheric and Crustal Sources

The following expression, $(NO_3^- + Cl^-)/ \sum-$, where $\sum-$ is the sum of the anions, can be used to assess the contribution of atmospheric and crustal sources of anions to glacial meltwater. Since halite is absent from the catchment (Tranter et al., 1997) it is assumed that there is no lithologic source of Cl^-. Therefore Cl^- represents the proportion of the anions that are atmospherically derived from the sea salt aerosol. The above calculation indicates the atmospheric component (anions) in the subglacial meltwater at HGA is approximately 6% of the total anion concentration inferring that a majority of the anions in the glacial meltwater are derived from crustal sources and not atmospheric sources. This expression also assumes that all NO_3^- is atmospherically derived from the acid nitrate aerosol and that there are no additional sources or sinks of NO_3^- (e.g., via nitrogen fixation). Subglacial meltwater contains a higher concentration of NO_3^- compared to supraglacial runoff and snow melt previously measured at HGA (Tranter et al., 1997) (Table 3.3), indicating a subglacial source of NO_3^- likely exists at HGA, and NO_3^- in meltwater is derived from other sources in addition to atmospheric input.

Marine Inputs

If it is assumed that the sea salt aerosol has the same composition as seawater itself, it is possible to calculate the solute input to the catchment using standard seawater ratios relative to Cl^- concentration for the major ionic species (Holland, 1978). Given

that the concentration of Cl^- is low in the streams (c. 2.8 μeq L^{-1}) the contribution of other ions (Na^+, K^+, Ca^{2+}, SO_4^{2-}, HCO_3^-) from the sea salt aerosol is likely negligible. Therefore a correction to compensate for marine inputs to subglacial meltwaters was not applied.

Atmospheric solute inputs at HGA can be measured via the chemical analysis of supraglacial water and snowmelt (Tranter et al., 1997). The mean concentrations of the dominant anions (HCO_3^-, SO_4^{2-}, and NO_3^-) and the dominant cations (Ca^{2+}, Mg^{2+}, Na^+, and K^+) contained in supraglacial runoff, snowmelt, and subglacial meltwater from HGA are shown in Table 3.3. Assuming that the concentration of solutes in snowmelt and supraglacial water at HGA have remained relatively consistent over each melt season, it is clear that atmospheric and supraglacial inputs of solute are negligible compared to the amount of solute generated in the subglacial environment.

Subglacial Sources of Nitrate

NO_3^- is present in snowmelt but not in icemelt in a number of glacial catchments (Tranter et al., 1994). The mean concentration of nitrate in HGA meltwater streams was 20.8 μeq L^{-1} (Table 3.3) which is higher than the average nitrate concentration in snowmelt and supraglacial runoff, 6.9 and 0.4 μeq L^{-1} respectively.

Table 3.3. Concentration of ions in supraglacial runoff, snow, and subglacial meltwater from HGA.

	Supraglacial runoff †	Snow †	Subglacial water ‡
Ca^{2+}	4.9	8.4	1085
Mg^{2+}	0.3	2.7	69.3
Na^{+}	0.2	1.3	21.2
K^{+}	0.2	0	16.9
Cl^{-}	1.2	3.8	2.4
NO_3^{-}	0.4	6.9	20.8
SO_4^{2-}	1.3	6.6	372
*HCO_3^{-}	4.2	•	789

Units are μeq L^{-1} for all ions
† Mean values from HGA supraglacial runoff and snow as reported in Tranter et al., 1997
‡ Mean values from water sampled from the left and right subglacial streams at HGA (October 2004)
* Calculated by charge deficit using PHREEQci (U.S.G.S.)
• No measurement taken

It is plausible that a lithologic source of nitrogen is present in the subglacial environment of HGA which results in waters with a high NO_3^{-} concentration. Holloway et al. (1998) showed that meta-sedimentary and meta-volcanic rocks contribute inorganic N to water in an alpine stream, resulting in increased concentrations of NO_3^{-} downstream. The dissolution of fixed N within muscovite layers may occur in zones of muscovite-rich meta-sedimentary rocks which underlie HGA and therefore a plausible source of inorganic N may exist and this source may contribute to the high concentration of NO_3^{-} in subglacial waters at HGA. Microbially fixed nitrogen in either the supraglacial or subglacial systems is another source that may contribute to the high concentration of NO_3^{-} in subglacial waters. Future investigations will address the source of nitrate in

subglacial meltwater by determining the isotopic composition of nitrate (i.e., $^{15}N\text{-}NO_3^-$ and $^{18}O\text{-}\ NO_3^-$). Nitrate derived from atmospheric inputs will have a different isotopic signature than nitrate from a lithologic or biologic source (Sebilo et al., 2003), making it possible to determine the origin of nitrate in the meltwater

Bacterial Populations in Meltwater and Subglacial Sediment

Microscopy revealed that microbes were present in glacial meltwater and sediment collected from the left and right subglacial streams at HGA. Total numbers of bacteria in subglacial meltwater ranged from $8.4 \times 10^3 - 1.3 \times 10^4$ cells mL^{-1} and in subglacial sediment total numbers of bacteria ranged from $3.6 \times 10^4 - 5.9 \times 10^4$ cells g^{-1} (Figure 3.1). The maximum number of bacteria was observed in the sediment sample collected from the left stream. In all samples, water and sediment, typical prokaryotic cell morphologies (i.e., cocci and bacillus) were observed. Actively dividing cells were also observed, and in many cases bacterial cells were attached to mineral grains. Stream water samples contained a substantial amount of fine-grained sediment which proved to be problematic when stained with SYBR Gold™ nucleic acid stain. Additional samples were stained with the nucleic acid stain DAPI nucleic acid stain due to the non-specific staining of mineral grains by SYBR Gold™. A comparison of the images revealed that use of DAPI resulted in a lower background staining of entrained sediment, which yielded a more accurate count of the bacterial cells in each sample. The results presented in this section are from samples stained with DAPI (Figure 3.1).

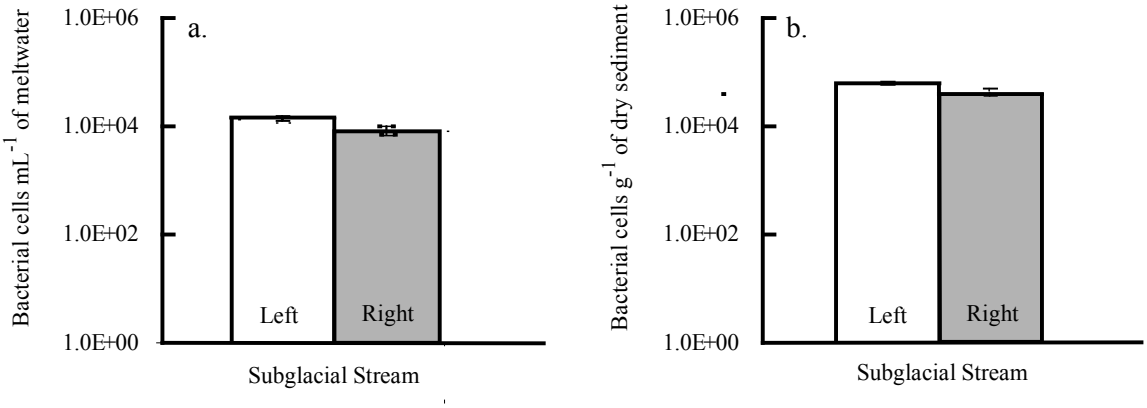

Figure 3.1. Total numbers of bacteria in water (a.) and sediment (b.) collected from the left and right subglacial streams at HGA. Error bars denote one standard deviation from the mean of triplicate counts.

16S rRNA Gene Sequences From Meltwater and Subglacial Sediment

Density gradient gel electrophoresis (DGGE) was used to compare partial 16S rRNA gene sequences amplified from Bacterial genomic DNA from HGA meltwater and subglacial sediment. The gel image (Figure A.1 in the Appendix) shows the similarity in banding patterns associated with sequences amplified from water and sediment samples from the left and right subglacial streams.

Bacterial clone libraries were constructed using 16S rRNA gene sequences amplified from genomic DNA extracted from meltwater and sediment from the left subglacial stream. Clones from meltwater (n=100) and sediment (n=85) were screened by restriction fragment length polymorphism (RFLP), and grouped into operational taxonomic units (OTU's) based on sequence similarity (6 OTU's for water and 10 OTU's for sediment). The clone library was dominated by sequences from bacterial groups such

as gamma and beta proteobacteria and *Cytophaga-Flavobacteria-Bacteroides* (CFB) (Figure 3.2).

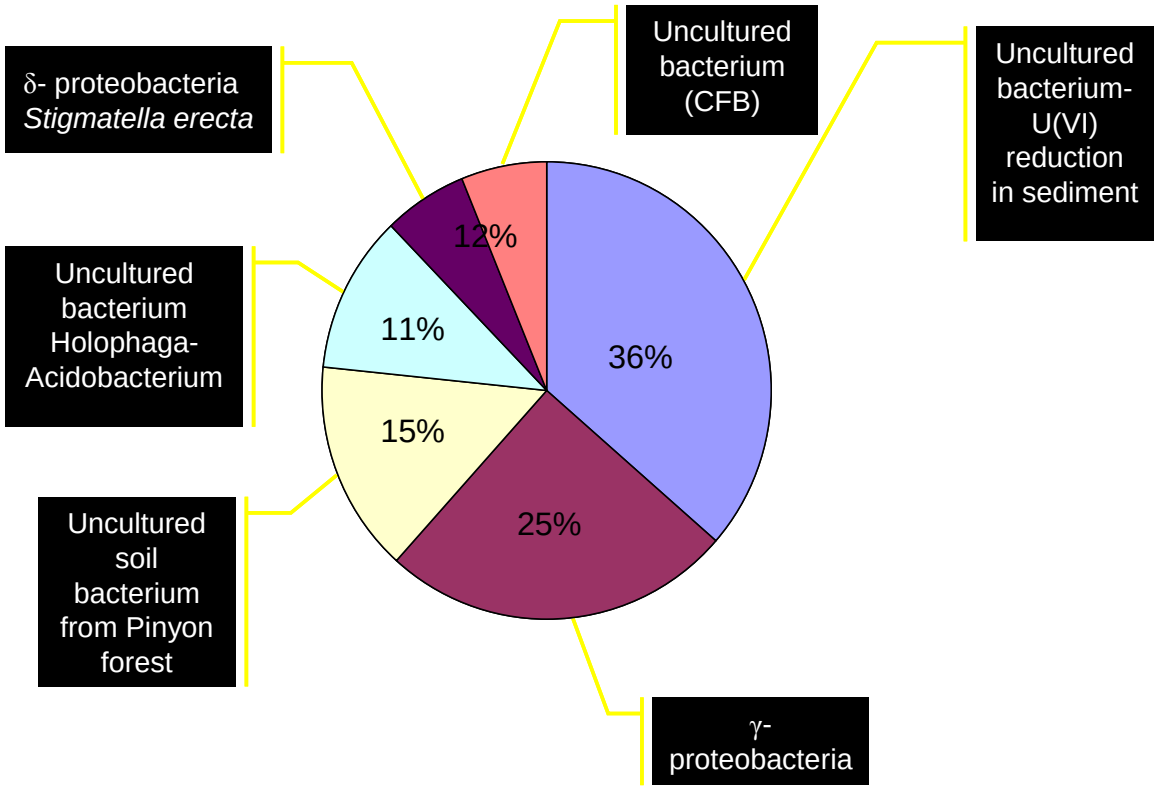

Figure 3.2. Bacterial DNA clone library. Results from analysis of 16S rRNA gene sequences of DNA clones (n= 100). Sequences were identified by BLAST search and indicated the closest neighbor based on 16S rRNA gene sequence.

Subglacial Heterotrophic Bacteria

Ten morphologically distinct bacterial colonies (named HGA-L-1 to 10) grew on R2A agar when inoculated with a glacial sediment / water slurry. Restriction enzyme digests of amplified DNA and analysis by RFLP yielded one distinct banding pattern

among the 10 isolates analyzed. The isolate (HGA-L-1) a representative of the 10, was cultured at 4°C and no growth was observed at 22°C. The partial 16S rRNA sequence of this isolate (HGA-L-1) was closely related (99%) to the psychrophilic bacteria *Flavobacterium xinjiangense* isolated from the China No. 1 glacier in Tibet (Zhu et al., 2003).

CHAPTER 4

MATERIAL AND METHODS

HGA Sediment Dissolution Experiment

4 L of water and 2700 g of sediment collected from the left subglacial stream of HGA were melted in an airtight plastic container under anaerobic conditions at < 4°C (Figure 4.1a). The melted sediment was homogenized in a pre-sterilized Fisher sampling bag (Fisher Scientific cat. no. 1176-2) and stored on ice in an anaerobic chamber. All manipulations (i.e., storage of the sediment, water, and bottles during the set-up) were performed on ice within the anaerobic chamber. Measured amounts of wet glacial sediment (40 g) and meltwater (70 mL) yielding a final sediment:water ratio of c. 0.57 g mL^{-1}, were dispensed into a pre-combusted (550°C) 100 mL glass serum bottle (Figure 4.1b) and each bottle was sealed with a Bellco© butyl stopper (Bellco Glass Inc., cat. no. 8748-B21) and aluminum crimp cap. The bottles were purged for 5 min with 0.1 μm filtered nitrogen or air to establish an anoxic or oxic headspace in the bottle. Termination of biologic activity in the killed control bottles was accomplished by chemical treatment with 0.2 μm filter sterilized pH buffered (7.0) formaldehyde or by autoclaving at 121°C for 30 min. Additional control bottles amended with the anaerobic indicator Resazurin were also prepared, and incubated in the same manner as the experimental bottles (Figure 4.1c.). Biotic test bottles and killed controls were incubated in the dark at c. 2°C (Figure 4.1d.) for 100 days.

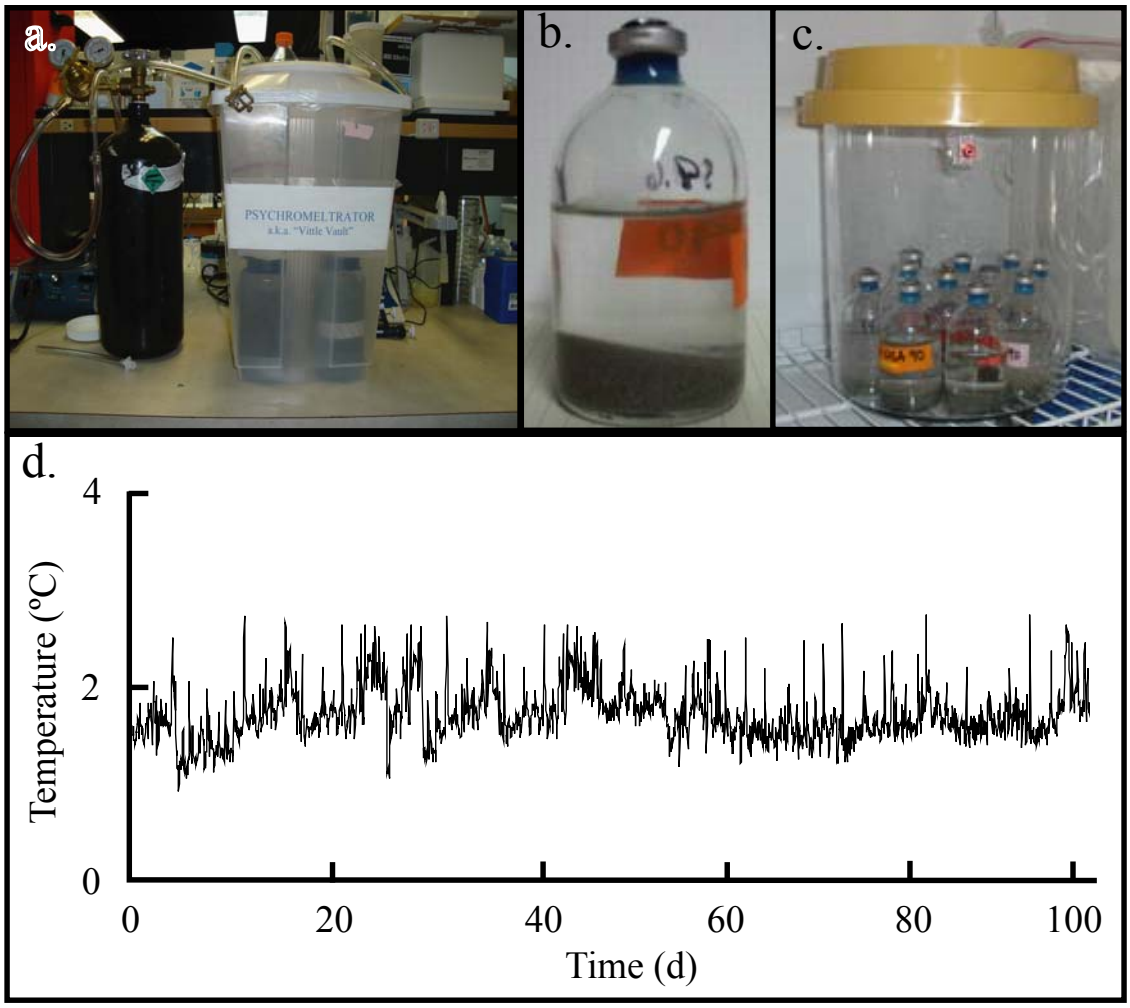

Figure 4.1. Laboratory Weathering Experiment. Sediments and water were melted under anaerobic conditions (a.) and dispensed into 100 mL serum bottles (b.) for incubation. Anoxic bottles were stored in Gas-Pak anaerobic containers (c.) and all bottles were incubated at ~2°C for the duration of the experiment (d.). Temperature was monitored using a probe inserted into a serum bottle containing water and this bottle was incubated alongside the experimental bottles. The probe was connected to a Campbell Scientific data logger (CS-10A) and the temperature of the water was recorded every 15 minutes.

Analyses of Bottle Contents

2 live bottles (oxic and anoxic) and 4 killed control bottles (2 heat killed and 2 chemically killed, oxic and anoxic) were sacrificed at each time point, (t = 0, 7, 14, 21,

28, 35, 45, 60, and 100 days). The 6 bottles were gently swirled and then re-incubated standing still for 10 min at 2°C to allow for settling. The aqueous contents of each bottle were extracted using a sterile 60 mL syringe (Becton, Dickinson and Co., cat. no. 309653) and 21 gauge needle. 40 mL of the aqueous contents were extracted from each bottle and filtered through a sterile 0.45 μm nylon filter (Fisher Scientific cat. no. 09-714) into a 20 mL scintillation vial rinsed 3x with filtrate and stored at < 4°C until analysis. 10.5 mL of the remaining aqueous portion was used for iron and sulfide colorimetric determinations, 3 mL and 7.5 mL respectively. pH was measured using a UB-10 bench top pH meter (Denver Scientific) and / or colorPHast indicator strips (pH range 6.0-10.0). Aqueous iron species and concentrations were determined using the Ferrozine colorimetric method (Ball et al., 2000) and sulfide concentrations were determined by methylene blue colorimetric assay (Franson, 1981). Spectrophometric measurements of Ferrozine and methylene blue were made with a USB-2000 spectrophotometer (Ocean Optics, Dunedin, Fl.). Dissolved oxygen (DO) in biotic and killed control bottles was measured at t=0 by Winkler titration (LaMotte Inc., U.S.A.). Dissolved gas species H_2 and CO_2 were determined in t = 100 d bottles using headspace gas chromatography (GC) analyzed with a Varian CP4900 Gas Chromatograph. The concentration of major cations (Ca^{2+}, Na^{+}, Mg^{2+}, NH_4^{+}, K^{+}), anions (F^{-}, Cl^{-}, NO_3^{-}, PO_4^{2-}, SO_4^{2-}), and organic acid anions (CH_3COO^{-}, $CHOO^{-}$), were determined by ion chromatography using the methods previously described in Chapter 2. The remaining bottle contents, sediment and water slurry were aliquoted into sub-samples to be used for additional analyses (i.e., microbial enumerations, microbial molecular analysis, and sediment characterization) and frozen at -80°C.

Direct Microscopic and Viability Counts

Total microbial cell counts and viable cell counts were performed on the sediment from biotic and killed control test bottles (t = 0, 35, and 100 d) using the nucleic acid stain DAPI, and the Live / Dead BacLight Bacterial Viability Kit (Molecular Probes, Inc., cat. no. L7007). The removal of cells from the sediment surfaces and the technique used to stain and filter the bacterial cells was performed as previously described in chapter 2, except DAPI stain was substituted for SYBR gold. The filtration and staining of bacterial cells from live (t = 100d) and killed control (t = 0 and 100d) bottles was performed at 4°C. The filter was covered with 200 uL of a solution containing 6 μmol L^{-1} of SYTO-9 stain and 30 μmol L^{-1} of propidium iodide and incubated for 15 minutes in the dark, as described by the manufacturer's protocol. The solution was vacuum filtered (25 kPa) and the filter was mounted on a glass microscope slide and visualized with epifluorescent microscopy using low fluorescence immersion oil. Cells on the filter were viewed and counted by the method previously described in chapter 2. The analysis of laboratory blanks stained with DAPI and Live/ Dead stains indicated that cellular contamination associated with sediment washing, staining, filtering, and microscopy were < 5 cells g^{-1} in all samples.

Genomic DNA Extraction from Sediment

DNA was extracted from the bacterial cells in the sediment from biotic test bottles (t = 0, 45, 60, 100 d) and autoclave killed control bottles (t = 0, 45, and 100 d) using a method modified from Bottomley (1994) for the removal of cells from soil for

enumeration. 10 g of wet sediment was added to a pre-combusted (550°C) flask containing 10 g of 3mm glass beads and 10 mL of 0.2 μm filter sterilized 0.15M NaCl. The sediment/glass bead slurry was swirled at 250 rpm for 20 min at < 4°C and the supernatant was poured into a 15ml mL Falcon™ tube. The tube was incubated for 15 minutes at 4°C to allow for the entrained sediment to settle. 10 mL of the aqueous contents were filtered onto a sterile 0.2 μm filter (Osmonics Inc., cat. no. 125-102) and the filter was placed in a 15 mL Falcon™ tube containing 3 mL of lysis buffer (Gordon and Giovannoni, 1996). Cellular nucleic acids were extracted from the filters with sequential phenol/chloroform (50:50) and phenol/chloroform/iso-amyl-alcohol (25:24:1) solutions and precipitated overnight in 0.1x vol. of 5M NaOAc and 2x vol. of 100% isopropanol. The extract was centrifuged, washed 3x with 70% ethanol, and dried in a laminar flow hood. The DNA was eluted in 100 μL of Tris EDTA (TE), and stored at -20°C.

PCR Amplification and Analysis of 16S rRNA Gene Sequences via DGGE

DNA extracted from the sediment of live bottles (t= 0, 45, 60, 100) was amplified using the Bacterial specific PCR/DGGE primers 1070F/1391GC (Muyzer et al., 1992). A nested PCR approach was used because traditional PCR with the primer set 1070F/ 1391GC resulted in low yields of amplified DNA. The nested PCR using the DNA oligonucleotide primers 27F/ 1492R was run under the following conditions , 90 seconds of initial denaturation at 95°C, 45 seconds of denaturation at 95°C, 30 seconds of annealing at 50°C (27F/1492R), and 90 seconds of elongation at 72°C for 10 cycles. The products from this reaction were re-amplified with the PCR/DGGE primers 1070/

1391GC under the following conditions: 45 seconds of initial denaturation at 95°C, followed by 45 seconds of denaturation at 95°C, 30 seconds of annealing at 54°C, and 90 seconds of elongation at 72°C for 25 cycles, and 5 minutes of final elongation at 72°C in a MJ Research PTC-200 thermalcycler. The products were run on a polyacrylimide gel as previously described in Chapter 2.

Mineral Characterization of Sediments

A combination of x-ray diffraction (XRD), scanning electron microscopy (SEM), and scanning electron microscopy/energy dispersive spectroscopy (SEM-EDS) were used to determine the bulk mineral composition and elemental composition of sediment grains from the live and killed control bottles (t = 0 and 100 days). The sediment was dried in an oven at 105°C and the dried sediment was ground into a powder using a mortar and pestle. The powder was analyzed by XRD on a Scintag X-ray Powder Diffraction Spectrometer (Image and Chemical Analysis Laboratory (ICAL), MSU). The X-ray spectra generated were analyzed manually using data reduction routines to determine peak position, relative intensities, and to calculate intracrystalline d-spacings. Peaks were then compared to the ASTM powder diffraction file for identification of unknown crystalline materials. For SEM analysis, the sediment samples were dried overnight at room temperature in sterilized ceramic crucibles. Sediment grains were mounted on an aluminum SEM stub using black sticky tabs, sputter coated with carbon to a thickness of 15 nm, and viewed on a JEOL 6100 Scanning Electron Microscope (ICAL, MSU). Ten fields were viewed for each sample, and pairs of secondary electron images and backscattered images were collected. Sediment grains in the ten fields of view were

randomly selected and analyzed using SEM-EDS to determine the elemental composition of the grain.

Acid Leach of Sediments for Calcite Concentration

Sediments from day 0 and 100 bottles (live and killed controls) were acid leached with 0.5N acetic acid at room temperature for 120 minutes to dissolve calcite and dolomite in sediment samples. The tubes were centrifuged for 3 minutes at 5,000 rpm and the leachate was decanted into a 60 mL syringe. The liquid was filtered through a 0.45 μm nylon filter into chromatography vials and diluted (1:100 and 1:1000) with 18.2 MΩ cm^{-1} water for analysis. The concentrations Ca^{2+}, Mg^{2+}, and Na^{2+} were measured using ion chromatography, by the methods described in Chapter 2.

CHAPTER 5

RESULTS

Subglacial Sediment Weathering Experiment

Bottle Headspace Gas Amendments

The concentration of dissolved oxygen (DO) in water from live and killed control bottles was measured (t = day 0) to assess the effect of the addition of headspace gases (air or nitrogen). Dissolved oxygen concentration of the water in live and killed controls flushed with sterile air (oxic) ranged from 7.8 - 8.1 mg L^{-1}, while bottles flushed with sterile nitrogen (anoxic) had values below the detection limit (< 0.1 mg L^{-1}). The waters in the bottles flushed with air were approximately 70% saturated with oxygen based on the calculation for oxygen saturation under laboratory conditions at MSU (10.4 mg L^{-1} @2°C and 1461 m a.s.l.).

Sterile Controls

The concentration of all aqueous chemical species measured from live and killed control bottles are listed in Table A.1 of the Appendix. This Table includes the results from the two different sterilization techniques used (heat and chemical). For this discussion only the results from the heat killed controls will be compared to the live incubations. Chemical sterilization of bottle contents by formaldehyde was effective at terminating the biologic activity in the bottles but modified the aqueous chemistry. In the

formaldehyde treated bottles the following differences were observed in the data, a) absence of the anion F^-, b) increased concentration of Cl^- (c. 12 μeq L^{-1}) compared to the live and killed bottles at Day 0. Formaldehyde treatments also resulted in the release of base cations (e.g., Ca^{2+} and Mg^{2+}) from the sediment, likely through acid dissolution since formaldehyde is readily oxidized to formic acid in the presence of oxygen.

Mineral Dissolution in Subglacial Sediment

Figure 5.1 shows the concentration of total dissolved solids (TDS) in live and heat killed control bottles over the incubation period. TDS is a measure of the solute concentration in water, and the results infer that solute generation from the reaction of subglacial meltwater and sediments is increased when microbes are present. Total dissolved solids in live bottles incubated under oxic conditions increased from 825 to 1400 μmol L^{-1} over 100 days, which was significantly greater than the increase in the killed controls (920 to 975 μmol L^{-1}). The greater proportion of solute generated in biotic laboratory dissolution experiments indicate that solute generating chemical reactions in subglacial sediments from HGA are enhanced in the presence of subglacial bacterial communities.

Figure 5.2 shows the changes in pH of the water from live and killed control bottles over the 100 day incubation. pH values of water in live and killed controls followed a similar trend over the experiment, with the exception of a slight increase (c. 0.4 units) in the live bottles (oxic and anoxic) from days 60-100.

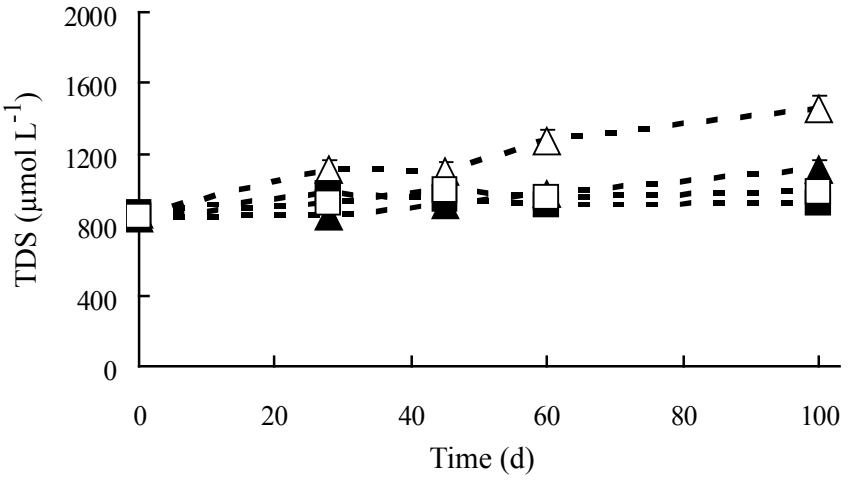

Figure 5.1. Total dissolved solids (TDS) measured in water from live and killed control bottles over the 100 day incubation. TDS in water from the live-oxic (open triangle) bottles increased 200% over the 100 day incubation compared to live-anoxic (solid triangle), killed-oxic (open square), and killed-anoxic (solid square) bottles. Error bars denote one standard deviation from the mean (n=3).

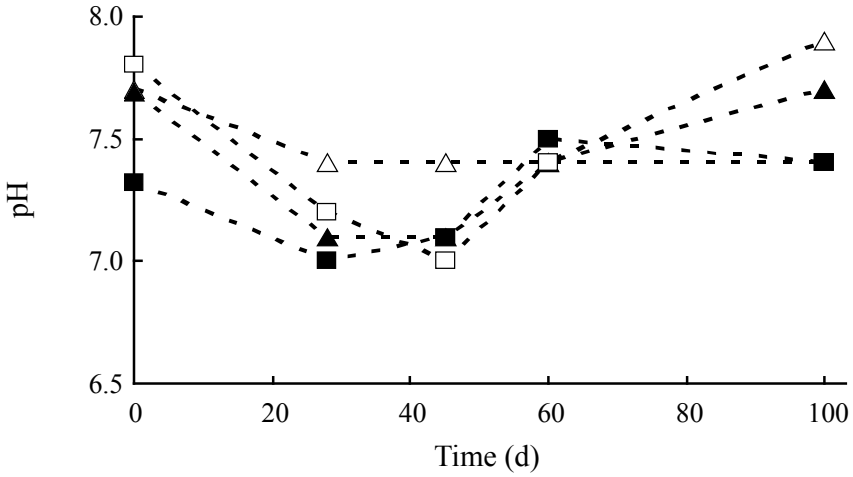

Figure 5.2. Changes in pH of water from experimental bottles. Shown: live-oxic (open triangle), live-anoxic (solid triangle), killed-oxic (open square), and killed-anoxic (solid square) bottles over the 100 day incubation period.

Microbially Enhanced Mineral Dissolution Under Oxic Conditions

Concentrations of major cations, anions, and organic acids in water from live and killed control bottles are shown in Table A.1 of the Appendix. Over the 100 day incubation period the dominant cation released into the water in the live bottles was Ca^{2+}, followed by Mg^{2+}, Na^{+}, and K^{+} in order of decreasing concentration. Relative increases in the aqueous concentration of Ca^{2+}, Mg^{2+}, and Na^{+} in the water from bottles in which biologic activity was allowed to persist (Figure 5.3) infers that under oxic conditions microbial activity increased mineral dissolution to produce these ions.

Figure 5.4 shows the relationship between $[Ca^{2+}]$ and $[*HCO_3^{-}]$ in water from live oxic bottles. The slope of the line plots near the 1:1 ratio ($y=0.9452x + 280.75$, $R^2 = .9984$) inferring that the evolved ratio of Ca^{2+} / $*HCO_3^{-}$ in the water component of the live oxic incubations is a result of carbonate dissolution (Tranter et al., 2002). The solid arrow denotes the Ca^{2+} intercept (280.75) which is not zero indicating an excess in Ca^{2+} over HCO_3^{-} which may be a result of additional Ca^{2+} released from the weathering of other minerals containing Ca^{2+} (e.g., apatite).

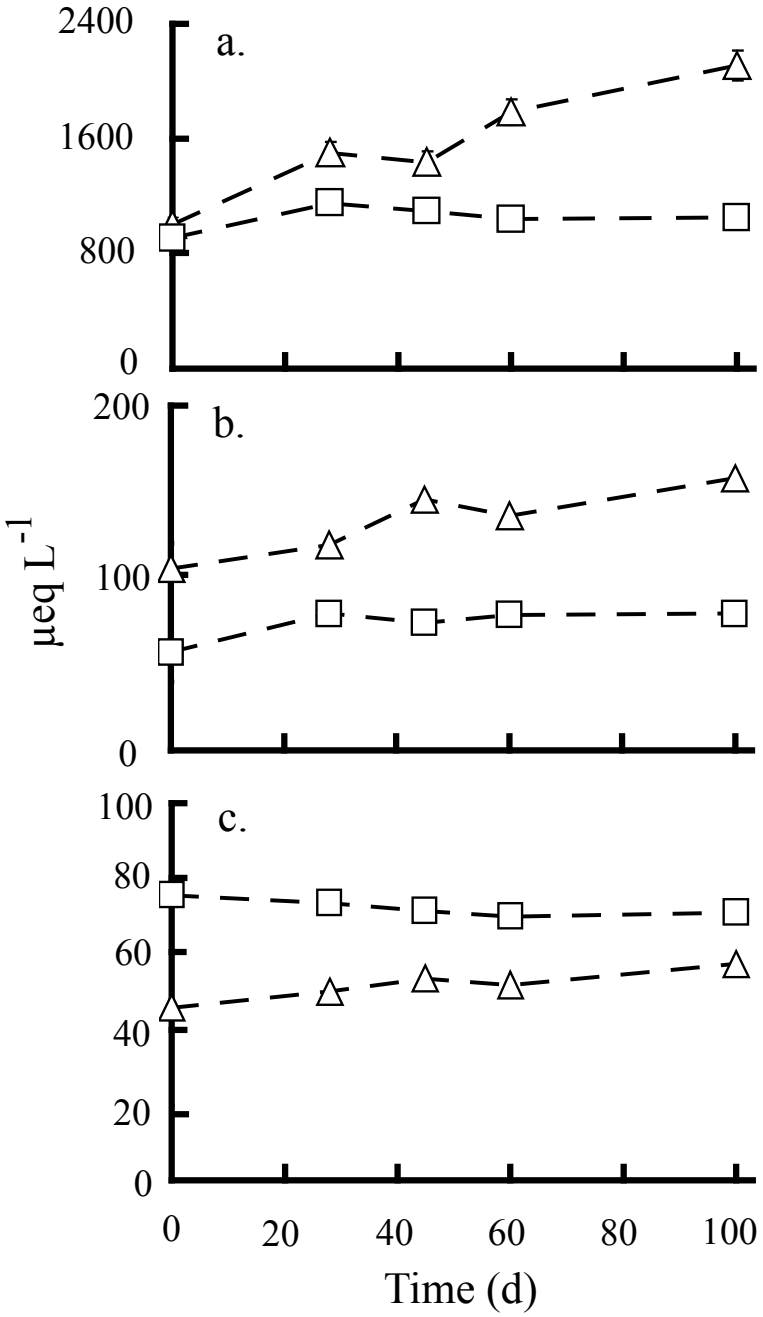

Figure 5.3. Concentrations of Ca^{2+} (a.), Mg^{2+} (b.), and Na^{+} (c.) in water from live-oxic (triangle) and heat killed control (square) bottles incubated under oxic conditions over 100 days. Error bars denote one standard deviation from the mean and are frequently within the size of the symbol.

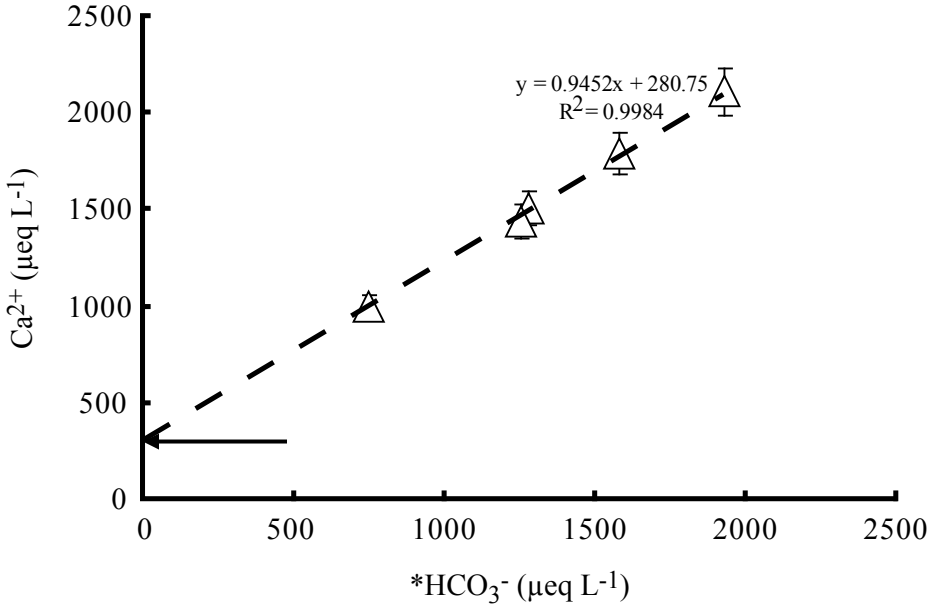

Figure 5.4. Plot of Ca^{2+} / $*HCO_3^-$ in water from live oxic incubations (days 0, 28, 35, 60, 100). The linear best-fit line shows the c. 1:1 ratio of Ca^{2+} / $*HCO_3^-$ in live bottles over the 100 day incubation.

Numerous studies have identified carbonate dissolution as a dominant solute generating reaction in subglacial environments of HGA and other temperate glaciers (Tranter et al., 1994, 2002, 2005; Skidmore et al., 2005). The dominant anion in the live and killed control oxic bottles over the 100 day incubation was $*HCO_3^-$, followed by SO_4^{2-} (Figure 5.5) and there was nearly a two-fold increase in the concentration of $*HCO_3^-$ in the live bottles relative to the killed controls.

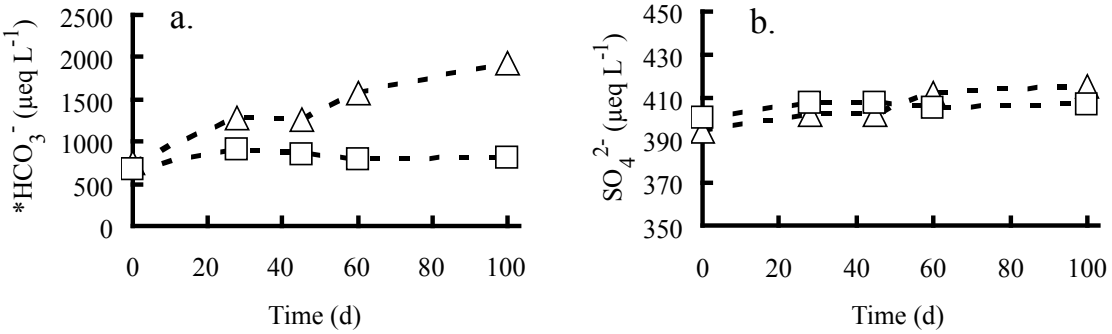

Figure 5.5. Concentration of $*HCO_3^-$ (a.) and SO_4^{2-} (b.) in live (triangle) and killed control (square) bottles over 100 days under oxic conditions. Error bars denote one standard deviation from the mean and in all cases are within the size of the symbol.

Nitrate Consumption Under Oxic Conditions

NO_3^- is a plausible source of energy for the bacterial communities in the subglacial environment at HGA. Figure 5.6 shows the decrease (c. 16 to 0 µeq L^{-1}) in NO_3^- concentration in the water from the live bottles over the first 35 days of the incubation. NO_3^- concentrations remained unchanged in the killed controls through day 35, and continued on the same trend until day 100 (complete data in Table A.1).

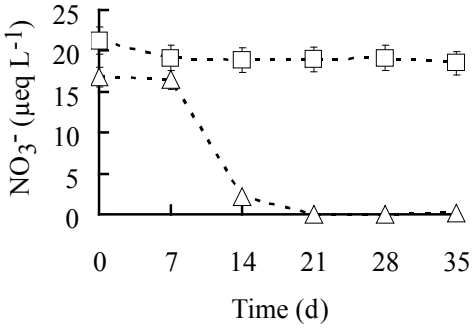

Figure 5.6. Concentration of NO_3^- in water from live (triangle) and killed control (square) bottles over the first 35 days of the experiment. NO_3^- concentrations in the live and killed controls remained constant from day 35 to day 100 (Table A.1). These results infer that nitrate is consumed under oxic conditions by bacteria in subglacial sediments.

Organic Acid Anions

The organic acid anions for acetic acid, acetate (CH_3COO^-) and formic acid, formate ($CHOO^-$) were detected in water extracted from the live and killed control bottles. The concentration of CH_3COO^- in live and killed control bottles is shown in Figure 5.7. Acetate concentrations in the live bottles reached a maximum concentration (5 μeq L^{-1}) at day 28 before declining to near zero at day 60 and remained at this level until the end of the experiment. Acetate concentrations in killed controls also showed a minor decline over the 100 days.

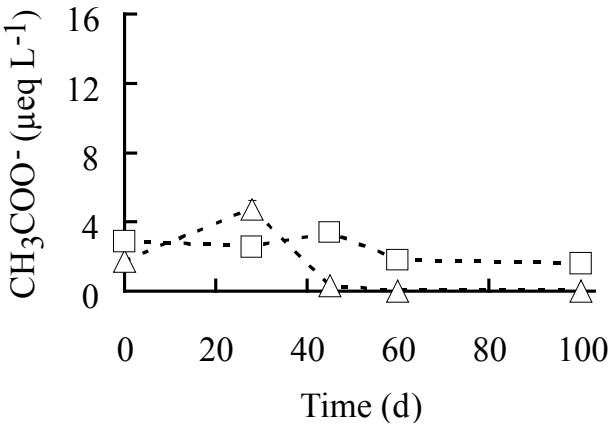

Figure 5.7. Concentration of organic acid anion, acetate (CH_3COO^-) in water from live-oxic (triangle) and killed control-oxic (square) bottles. Error bars denote one standard deviation from and in all cases they fall within the size of the symbol.

Microbially Enhanced Dissolution Under Anoxic Conditions

The generation of solute in live anoxic bottles was considerably less (+333 μeq L^{-1} of Ca^{2+}) than the amount of solute generated under live oxic conditions (+1100 μeq L^{-1} of Ca^{2+}) (Figures 5.3 and 5.8). Concentrations of major cations, anions, and organic

acids in water from the anoxic live and killed control bottles are shown in Table A.1. Over the 100 day incubation period the dominant cations released into the water in the live bottles were Ca^{2+} and Mg^{2+} and the dominant anions were $*HCO_3^-$ and SO_4^{2-}. In the anoxic incubation bottles, biological activity did not increase the quantity or rate of solute released into the water during the experiment (Figure 5.8). These results infer that the release of major cations (e.g., Ca^{2+} and Mg^{2+}) via mineral dissolution by biotic and abiotic processes in this experiment are similar under anoxic conditions, and are not enhanced when bacteria are present.

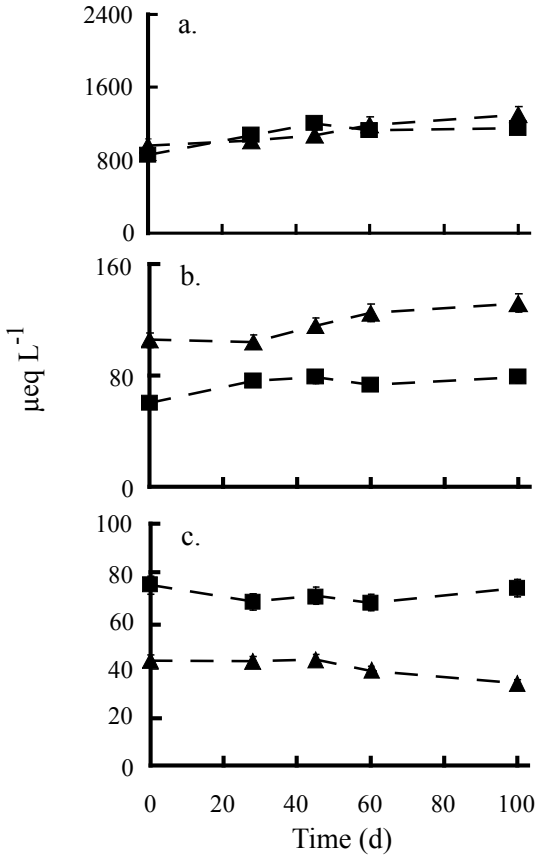

Figure 5.8. Concentration of Ca^{2+} (a.), Mg^{2+} (b.), Na^{2+} (c.) in water from anoxic live (triangle) and anoxic killed control (square) bottles over 100 days. Error bars denote one standard deviation from the mean and in many cases are within the size of the symbol.

Nitrate Consumption Under Anoxic Conditions

The concentration of NO_3^- in the live vs. killed control bottles incubated under anoxic conditions is shown in Figure 5.8. The NO_3^- concentration remained at c. 18 ueq L^{-1} through day 35 in the killed controls, and continued to remain at this concentration for the duration of the experiment while NO_3^- concentrations dropped to near zero in the live bottles by day 14. The majority of the nitrate had been consumed in the live-anoxic bottles by day 14 whereas in the oxic bottles nitrate was present until day 21 (Figures 5.6 and 5.9). The results indicate that NO_3^- is consumed when microbes are present. In anoxic bottles NO_3^- depletion does occur during the first 7 days and is complete by day 14 whereas the NO_3^- depletion in the oxic bottles starts at day 7 and is complete by day 21.

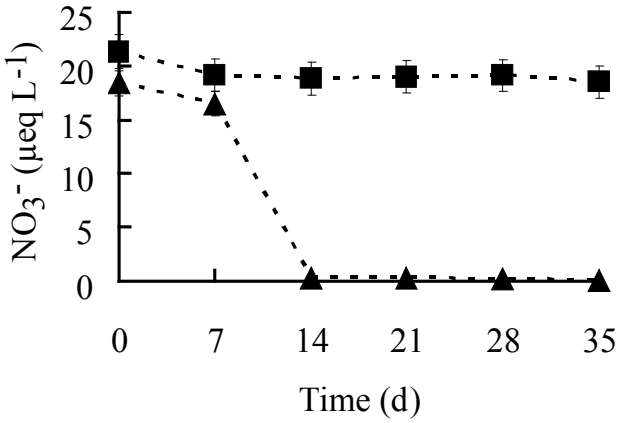

Figure 5.9. Concentration of NO_3^- in live (triangle) and killed control (square) bottles incubated under anoxic conditions. After 35 days the concentration of NO_3^- remained constant until the end of the experiment (Table A.1). Error bars denote one standard deviation from and in many cases they fall within the size of the symbol

Organic Acid Anions

The concentration of $CHOO^-$ decreased in the live bottles (2.1 to 0 μeq L^{-1}) and remained relatively constant (1.6 -1.3 μeq L^{-1}) over 100 days (Figure 5.10). The concentration of CH_3COO^- increased in the water from the live bottles beginning on day 28, and increasing to a maximum concentration (138.1 μmol L^{-1}) at day 100 (Figure 3.9). There was a greater net increase in CH_3COO^- over the 100 days in the live bottles (+138.1 μmol L^{-1}) compared to the killed controls (+2.0 μmol L^{-1}). Two explanations for this increase are by bacterial acetogenesis which is only catalyzed by groups of strict anaerobes which grow chemolithotrophically through the reduction of CO_2 to acetate using H_2 as an e- donor (Madigan et al., 2003) or the breakdown of larger organic molecules by bacteria which is more likely given the lack of free H_2 in the system (Figure A.2 in the Appendix).

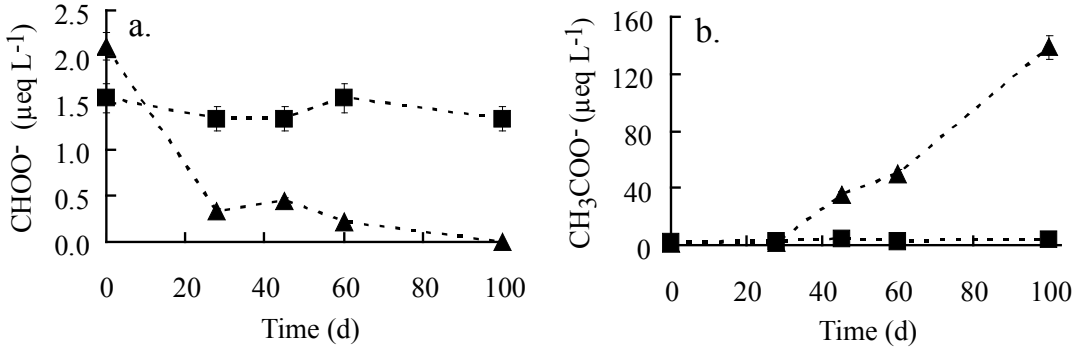

Figure 5.10. Concentration of formic acid (a.) and acetic acid (b.) in live (triangle) and killed control (square) bottles incubated under anoxic conditions. Error bars denote one standard deviation from and in all cases they fall within the size of the symbol.

Aqueous Iron in Anoxic Sediment Incubations

A greater concentration of Fe^{2+} was generated in the biologically active bottles relative to the killed controls over the 100 day incubation. The increase in concentration of aqueous Fe^{2+} (0.0 – 5.0 μmol L^{-1}) in the live bottles is attributed to biologic activity since there is only a negligible change in the concentration of Fe^{2+} in the killed controls, as shown in Figure 5.11.

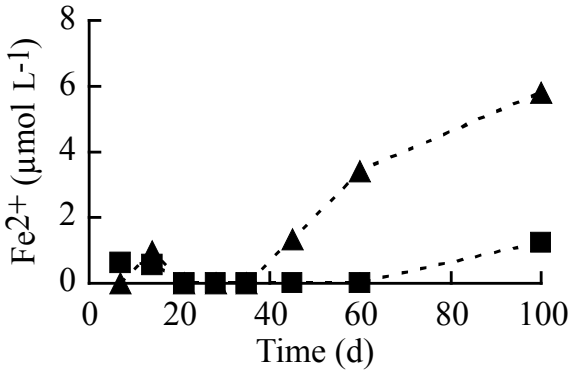

Figure 5.11. Concentration of Fe^{2+} in live (triangle) and killed control (square) bottles incubated under anoxic conditions. Error bars denote one standard deviation from the mean and in all cases errors lie within the size of the symbol.

Dissolution of Carbonate in Sediments

Acetic acid leaching of sediments from live and killed control bottles was performed in order to demonstrate that sufficient and broadly equal amounts of carbonate were present in all bottles (e.g., anoxic, oxic and live and killed controls). The results of this experiment are shown in Figure 5.12 and these results indicate that all experimental

bottles (Day 0 and 100) contained a considerable amount of carbonate available for dissolution (>15 meq L^{-1} of Ca^{2+} released from all sediments).

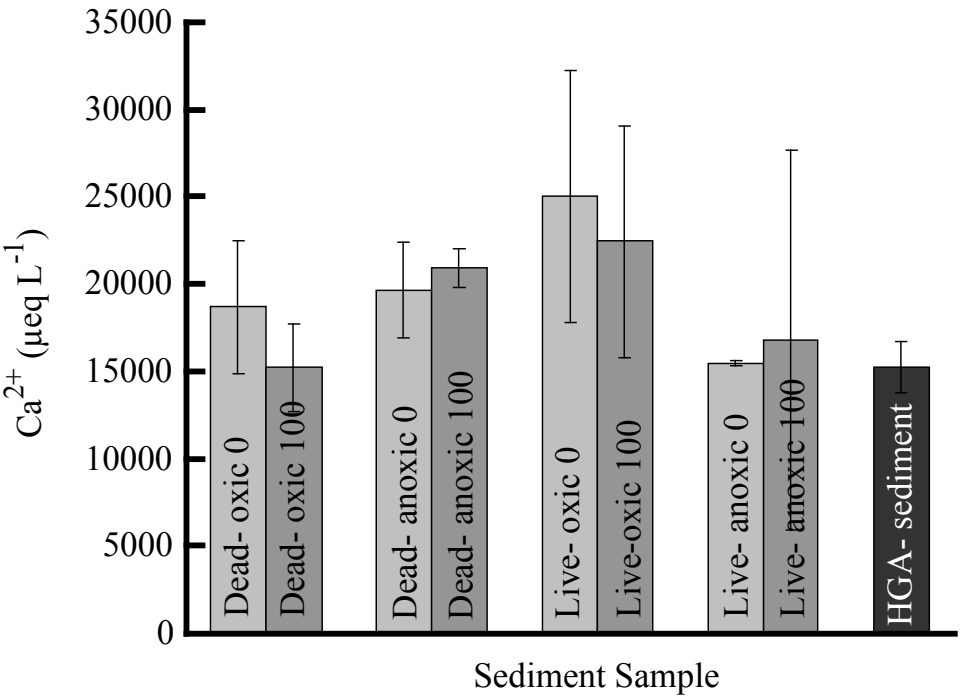

Figure 5.12. Concentration of Ca^{2+} liberated from sediments after digestion with 0.5M acetic acid for 120 minutes. Error bars denote one standard deviation from the mean of triplicate analyses.

Microbiological Analyses of Sediment Bacteria

Enumeration of Bacterial Cells

There was no significant increase in bacterial cell numbers in the live bottles over the 100 day incubation period. Total cell numbers in live oxic and anoxic bottles from day 0 were 3.5 x 10^4 cells $g^{-1}$and 4.2 x 10^4 cells g^{-1} respectively. Cell numbers increased

in day 35 oxic and anoxic bottles (Figure 5.13) and day 35 anoxic sediments contained the highest number of cells (1.1 x 10^5 cells g^{-1}) of the samples analyzed (days 0, 35, and 100).

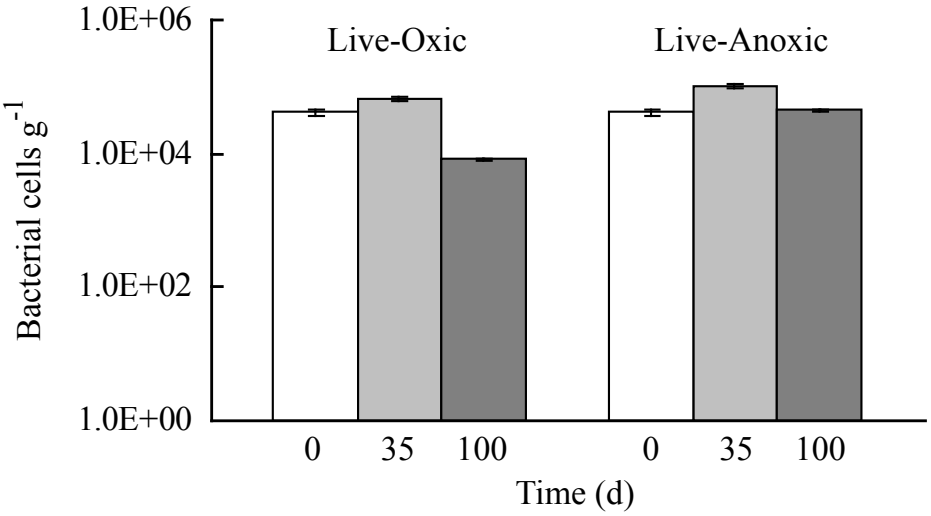

Figure 5.13. Total counts of bacterial cells per gram of dry sediment from live oxic and anoxic bottles. Error bars denote one standard deviation from the mean.

The results from live-dead staining of bacterial cells in the killed control bottles are shown in Table A.2 of the Appendix. A higher percentage of cells were lysed by heat sterilization in the oxic bottles (98%) compared to the anoxic (93%). Despite a small percentage of live stained cells in the killed controls at day 0, all killed control bottles were assumed to exhibit negligible biologic activity throughout the experiment since concentrations of NO_3^- in all killed bottles remained unchanged. Sediment from a live incubation bottle (day 0) was stained using live-dead stain. This sample provided a positive control for the live/dead staining technique and a general idea of the proportion of live/ dead cells in the bottle after 100 days (Table A.2).

Denaturing Gradient Gel Electrophoresis

The gel image from denaturing gradient gel electrophoresis (DGGE) of amplified partial 16S rRNA sequences from the sediment of live oxic and anoxic bottles (day 0, 45, 100) is shown in the Appendix (Figure A.1). Changes in banding pattern, highlighted by the boxes, in samples from oxic and anoxic bottles indicate that there was a change in community composition, based on SSU 16S rRNA gene sequence, over the 100 days.

CHAPTER 6

DISCUSSION

Subglacial Biogeochemistry

Meltwater Chemistry

The concentration of NO_3^- in subglacial meltwater collected from HGA was considerably higher (~20 μeq $L^{-1,}$ Table 3.3) than the average NO_3^- concentration in snowmelt and supraglacial runoff previously measured at HGA (Tranter et al., 2002). Three types of concentrated subglacial water (Type A, B, C) have been identified at HGA by the chemical analysis of borehole water (Tranter et al., 2002). Type B waters have NO_3^- concentrations of ~10 μeq L^{-1} which are greater than the concentrations in snowmelt and supraglacial runoff and are representative of waters flowing through an efficient distributed drainage system. The concentration of NO_3^- and time frame of sampling (late-season) leads to the conclusion that the waters collected for this study represent waters flowing through a distributed drainage system at the glacier bed.

The concentration of SO_4^{2-} in the water samples collected for this study ranged from 335 μeq L^{-1} – 409 μeq L^{-1}. These results indicate that the waters were unlikely to have flowed through a fully anoxic system at the glacier bed since the concentrations are slightly below 414 μeq L^{-1}, which is the upper limit of SO_4^{2-} that can be generated via closed system oxidation of sulfide by oxygen saturated water (Tranter et al., 2002). However, it is possible that more concentrated waters from such an anoxic environment

may have mixed with dilute supraglacial waters to give the observed outflowing water concentrations.

Subglacial Microbiology

Free floating bacterial cells in meltwater may originate from a variety of environments; sediment and basal ice surfaces at the base of the ice in distributed drainages, debris-rich basal ice and sediment beds in channelized drainages, the channel marginal zone, or delivered from the surface of the glacier, directly into a channelized drainage system. Bacteria found in sediment pools in the meltwater stream may colonize the sediments after they are deposited, or the cells may have remained attached to the sediment grains which are transported and deposited in shallow pools in the meltwater stream. Viable bacterial cells were isolated on R2A media and microscopy revealed bacterial cells in fixed water samples, which were actively dividing. Sharp et al. (1999) also showed that HGA subglacial meltwater contained cells which were assumed to be active since 5%- 25% of the cells counted were either dividing or had recently divided. The total number of bacterial cells in subglacial meltwater from HGA ranged from 8.4 x 10^3 – 1.3 x 10^4 cells mL^{-1}, and in subglacial sediments 3.6 x 10^4 – 5.9 x 10^4 cells g^{-1}. These measurements are lower than previous measurements of cell biomass in subglacial meltwater (2.0 x 10^5 cell mL^{-1}) and sediments (1.5 x 10^7 cells g^{-1} to 2.1 x 10^8 cells g^{-1}) from HGA by Sharp et al. (1999). Differences in total counts of bacterial cells from water and sediment samples in this study and Sharp et al. (1999) are likely related to the nature of the samples collected. In contrast to previous work at HGA (e.g., Sharp et al., 1999) this study used additional techniques, i.e. cultivation on growth media,

construction of DNA clone libraries, sequencing of 16S rRNA genes, and analysis of 16S rRNA gene sequences by DGGE) to investigate the populations of bacteria in subglacial sediments and meltwater from HGA.

Viable bacterial colonies from water and sediment were grown on heterotrophic media (R2A agar) at temperatures of 4°C and 22°C and 10 isolates were examined. RFLP analysis of PCR amplified 16S rRNA gene sequences from each isolate indicated that 9 out of 10 possessed similar SSU rRNA gene sequence. Isolate HGAL-L-1 possessed a unique RFLP pattern and grew at 4°C as a yellow to orange pigmented cell, with rounded colonies, and would not grow at 22^{o}C on the R2A agar. The partial (~1100 bp) 16S rRNA gene sequence of this isolate (HGAL-L-1) was closely related (99% similarity) to the psychrophilic bacteria *Flavobacterium xinjiangense* sp. nov. isolated from frozen soil at China No.1 glacier in Tibet (Zhu et al., 2003). *Flavobacterium xinjiangense* was well characterized by Zhu et al. (2003) and is strictly aerobic, psychrophilic, non-flagellated, and nongliding. Colonies are pale yellow, circular and smooth. This organism is heteroorganotrophic and was able to utilize glucose, cellobiose, maltose, fructose, sucrose, arabinose and xylose as sole carbon sources and this organism did not reduce nitrate (Zhu et al., 2003).

Banding patterns from DGGE analysis of partial 16S rRNA gene sequences amplified from sediments and water samples collected from the subglacial streams infer the microbial community composition of sediments and water from HGA is different (Figure 5.14). Yet little difference was observed in the banding pattern between samples collected from the left and right streams which indicate a degree of homogeneity in subglacial communities in both streams (Figures 5.14 and A.1). These results, and the

results of chemical analysis of waters flowing from both streams infer that subglacial waters from the left and right stream are likely similar in origin, have a similar residence time, and similar routing through the subglacial system.

Laboratory Weathering Experiment

Laboratory incubations of subglacial sediment and water conducted at near freezing temperatures (~ 2°C) indicates that solute concentrations increase (e.g., ~1100 μeq L^{-1} for Ca^{2+}) under oxic to sub-oxic conditions when bacteria are present. A gradient of oxic to sub-oxic conditions within the sediments is likely to have developed since the sediments were not constantly flushed with water and re-oxygenated. The formation of a gradient is likely due to the consumption of dissolved oxygen in sediment pore waters by bacteria, which results in the formation of oxic and sub-oxic microzones. Similarly, sub-oxic to anoxic microzones likely exist in the sediment beds at the base of the glacier (e.g., Bottrell and Tranter 2002) and in the sediments found in the meltwater stream. The experiment used meltwater and sediment from a subglacial stream draining HGA which contains the native populations of bacteria from the subglacial environment and the same nutrients and energy sources available to these organisms in their natural environment. Therefore, it is likely that microbial activity and microbially-mediated mineral dissolution observed over the course of this experiment is analogous to processes which occur in the subglacial environment of HGA. Previous laboratory investigations into the weathering of subglacial sediments by Sharp et al. (1999) and Kivimäki (2005) showed that bacteria do impact chemical weathering processes such as sulfide oxidation (e.g., Sharp et al., 1999) or the dissolution of silicate minerals under oxic conditions (e.g.,

Kivimäki 2005). This study investigated the rates of mineral dissolution by biotic and abiotic processes under oxygenated conditions and strictly anoxic conditions, which were not tested in the experiments conducted by Sharp et al., (1999) and Kivimäki (2005).

Carbonate dissolution is believed to be one dominant weathering reaction which occurs in the subglacial system of HGA (e.g., Tranter et al., 2002). The predominant ions released into solution when bacteria were present were Ca^{2+}, $*HCO_3^-$, and Mg^{2+} in order of decreasing concentration. The mean concentration of Ca^{2+} released over the incubation period in the live bottles (1105 μeq L^{-1}) was significantly greater (148 μeqL^{-1}). Statistical analysis (t-test) of the slopes of the change in the concentration of dissolved species (Ca^{2+}, Mg^{2+}, Na^+, and SO_4^{2-}) in live and killed control bottles over the 100 day incubation is shown in Table A.3 of the Appendix. Saturation indices (SI) for $CaCO_3$ (calcite) in waters from oxic, live and killed control bottles were calculated using PHREEQci (Parkhurst, 1995). The SI for calcite in waters from live bottles at day 100 was -0.16 and in killed controls -1.30. These results indicate that the waters from the killed controls remained undersaturated with respect to calcite, whereas by day 100 waters from the oxic live bottles were nearing saturation with respect to calcite. The reason for the degree of undersaturation in the killed controls compared to the live bottles is unclear but these results do infer that waters reach conditions close to saturation with respect to calcite in a shorter time under oxic to sub-oxic conditions when bacteria are present.

Previous work by Sharp et al. (1999) and Tranter et al. (2002) determined that the predominant weathering reactions in the subglacial environment of HGA were sulfide oxidation coupled to carbonate dissolution and carbonate dissolution is believed to be

driven by protons produced from sulfide (FeS_2) oxidation (e.g., Sharp et al., 1999; Tranter et al., 1997, 2002). The oxidation of sulfide when coupled to carbonate dissolution, gives SO_4^{2-}: HCO_3^- ratios of 1:1 (in equivalents). The ratio of SO_4^{2-}: HCO_3^- in the live oxic bottles ranged from 0.3 - 0.5 due to an excess of HCO_3^- and small increases (21 μeq L^{-1}) in SO_4^{2-}. The calculation of SO_4^{2-}: HCO_3^- ratios in live and killed control bottles is shown in Table A.4 of the Appendix. These results infer the coupling of sulfide oxidation to carbonate dissolution was not the dominant solute producing reaction during the experiment. This conclusion is interesting because it implies that carbonate dissolution in subglacial sediments from HGA still occurs even when the reaction is not driven by protons released via the oxidation of sulfide. Under experimental conditions carbonate dissolution was clearly driven by bacterial activity. These results exemplify the importance microbial activity has on the production of CO_2 in basal sediments in the subglacial environment. A consequence of the production of CO_2 by respiring bacteria is the weathering of minerals since the CO_2 produced dissolves to form carbonic acid producing dissolution of carbonates.

The amount of Ca^{2+} released under oxic to sub-oxic conditions was nearly 8 times greater by biotic processes than by abiotic processes over the 100 day incubation. These results are further evidence that microbial activity has a major contribution to carbonate dissolution and this activity is likely an important process in the weathering of sediment under oxic to sub-oxic conditions in the subglacial environment of HGA.

The concentration of NO_3^- in live bottles under oxic conditions did not change during the first seven days of the experiment (Figure 5.6). During this time bacterial activity was solely via aerobic respiration and used oxygen as the sole terminal electron

acceptor, hence no NO_3^- was consumed. Whereas, under anoxic conditions NO_3^- depletion occurred over the first seven days, inferring bacterial anaerobic respiration using NO_3^- as a terminal electron acceptor. The usage of NO_3^- by bacterial respiration also indicates that the bottles were initially anoxic and remained anoxic over the 100 days. Furthermore, the depletion of NO_3^- by day 21 (Figures 5.6 and 5.9) and marked increase in the concentration of Fe^{2+} beginning at day 35 in "live" bottles under anoxic conditions (Figure 5.11) was evidence of the establishment of a natural redox gradient (Stumm and Morgan, 1996) in the sediments over time.

No significant changes in the magnitude of mineral dissolution were observed between the biotic and abiotic incubations under anoxic conditions (Figures 5.3 and 5.8). However, the concentration of acetate in live bottles increased by two orders of magnitude over the 100 day incubation relative to the killed controls under anoxic conditions (Figure 5.10). Acetate is a potential carbon source for heterotrophic bacteria in the sediments under oxic conditions. Therefore, as waters migrate from anoxic zones to sub-oxic to oxic zones at the glacier bed a potential carbon source (i.e., acetate) becomes available for aerobic heterotrophs.

The changes in concentrations of Ca^{2+} (presumably resulting from heterotrophic activity) under oxic conditions, depletion of NO_3^- under oxic and anoxic conditions, and the production of acetate and Fe^{2+} under anoxic conditions suggests that a consortia of metabolically active bacteria were present in the sediments (Figure 6.1). Thus it seems reasonable to infer that there is a consortium of metabolically diverse bacteria in the basal sediments at HGA that are active under the appropriate redox conditions.

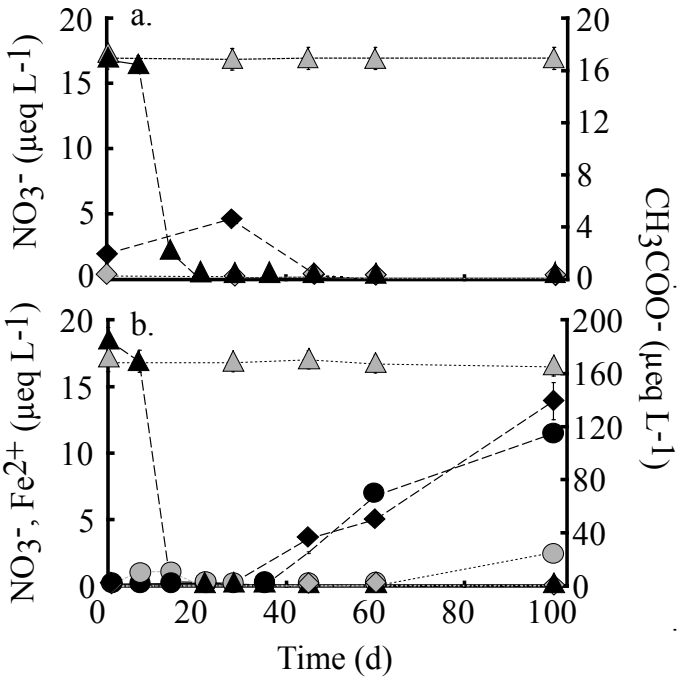

Figure 6.1. Chemical evidence of microbial activity in subglacial sediments under oxic and anoxic conditions at 2°C. Under oxic conditions (a.), microbial activity results in decreases in the concentrations of NO_3^- (black triangle) and CH_3COO^- (black diamond) compared to killed controls (grey triangle and grey diamond). Under anoxic conditions (b.) NO_3^- concentration decreased to zero in live (black triangle) anoxic bottles after 21 days whereas no change occurred in NO_3^- concentration in the killed controls (grey triangle). Following the decrease in concentration of NO_3^- to zero (day 21) there was an increase in the concentration of Fe^{2+} (black circle) relative to the killed controls (grey circle). In the live anoxic bottles (black diamond) the concentration of CH_3COO^- increased by 140 μeq L^{-1} over the 100 day incubation and this increase was ~100 times greater than the amount generated in the killed controls (grey diamond).

Geomicrobiology of HGA

Cell biomass (Figure 5.13), measured as the total number of bacterial cells per gram of dry sediment, remained relatively stable over the course of the experiment. The sediments used for cell enumeration were sampled from different bottles and therefore some difference in cell biomass was expected, e.g. cell biomass in t = 100 bottles is unknown at t = 0. Furthermore, the sediments incubated were unamended with media

and nutrients and for this reason it is unlikely that a large change would occur in the population size over 100 days.

A change in the bacterial community structure over the 100 days was determined by DGGE of partial 16S rRNA gene sequences (Figure 5.14). Waters for this study were collected during the melt season when surface water inputs to the subglacial system are low and declining since the start of October is the end of the melt season. DGGE patterns from field samples show differences in 16S rRNA gene sequences amplified from subglacial waters and sediments. The subglacial waters we sampled for this study likely contain populations of allochothnous bacteria which were delivered to the subglacial environment and flushed out via the meltwater stream. Over time autochothnous populations of bacteria, most likely from the sediments, emerge and these populations will begin to dominate the community composition of the subglacial sediments. Evidence for this change is supported by the differences in banding pattern on the DGGE gel shown in Figure 5.14. Interestingly, the predominant OTU's at day 100, depicted by band presence and intensity, are not the same as day 0, and this change is likely a result of the closed-system nature of this experiment which introduced biologically limiting factors (i.e., nutrients and dissolved O_2). In distributed drainages at the glacier bed similar nutrient limiting conditions may also exist which result in organisms that dominate the subglacial bacterial community.

Broader Implications

The results from the aqueous chemical analysis of field samples and mineral dissolution experiments conducted in the laboratory indicate that carbonate dissolution is

the dominant solute generating reaction in the subglacial environment of HGA. Most notably, there is strong evidence from our experiments this process is enhanced by bacteria under oxic conditions. Furthermore, our laboratory experiments indicate a biogeochemical link exists between anoxic and oxic environments which co-exist in subglacial sediments. The biogeochemical weathering processes in the subglacial environment are an important component of the Earth system due to the magnitude of terrestrial ice cover over geologic time and the likelihood that bacteria were an important component of the terrestrial biosphere during these glaciations. Continental ice cover is currently 11%, rising to 30% during the Pleistocene glaciations (Knight, 1999) and near 100% during the pervasive low latitude glaciations in the Neoproterozoic (Kirschvink, 1992). Recent work indicates the presence of subglacial water at the bed of larger contemporary ice masses, e.g., Greenland and East Antarctica (Anderson et al., 2004; Dowdeswell and Siegert, 2002). Where wet based ice sheets exist one would expect microbial activity, thus the deep cold biosphere and biogeochemical cycling in these regions may be greater than previously thought.

REFERENCES

Altschul, S.F., Gish, W., Miller, W., Myers, E.W. & Lipman, D.J. (1990) "Basic local alignment search tool." Journal of Molecular Techniques. **215**:403-410.

Andersen, K.K, Azuma, N., Barnola, J.-M., Bigler, M., Biscaye, P., Caillon, N., Chappellaz, J., Clausen, H.B., Dahl-Jensen, D., Fischer, H., Fluckiger, J., Fritzsche, D., Fujii, Y., Goto-Azuma, K., Grønvold, K., Gundestrup, N.S., Hansson, M., Huber, C., Hvidberg, C.S., Johnsen, S.J., Jonsell, U., Jouzel, J., Kipfstuhl, S., Landais, A., Leuenberger, M., Lorrain, R., Masson-Delmotte, V., Miller, H., Motoyama, H., Narita, H., Popp, T., Rasmussen, S.O., Raynaud, D., Rothlisberger, R., Ruth, U., Samyn, D., Schwander, J., Shoji, H., Siggard-Andersen, M-L., Steffensen, J.P., Stocker, T., Sveinbjörnsdottir, A.E., Svensson, A., Takata, M., Tison, J.-L., Thorsteinsson, TH., Watanabe, O., Wilhelms, F., White, J.W.C. (2004). "High-resolution record of Northern Hemisphere climate extending into the last interglacial period." Nature 431: 147-151.

Anderson, S. P., Drever, J.I., Humphrey, N.F. (1997). "Chemical weathering in glacial environments." Geology 25(5): 399-402.

Anderson, S. P., Drever, J.I., Frost, C.D., Holden, P. (2000). "Chemical weathering in the foreland of a retreating glacier." Geochimica et Cosmochimica Acta 64(7): 1173-1189.

Arnold, N., Richards, K., Willis, I., Sharp, M.J. (1998). "Initial results from a distributed, physically based model of glacier hydrology." Hydrological Processes 12: 191-219.

Ball, J. W., Nordstrom D.K., McCleskey, R.B., To, T.B. (1999). "A New Method for the Direct Determination of Dissolved Fe (III) Concentration in Acid Mine Waters." USGS Publications 1: 1-10.

Benn, D.I., Evans, D.J.A. (1998) "Glaciers and Glaciation." London, UK, Arnold.

Bottomley, P.J. (1994). "Light microscopic methods for studying soil microorganisms. In Methods of Soil Analysis", Part 2 (Weaver, R.W, Angle, S., Bottomley, P., Bezdicek, D., Smith, S., Tabatabai, A., and Wollum, A., Eds.), pp. 81—105. Soil Science Society of America, Madison, WI.

Bottrell, S. H., Tranter, M. (2002). "Sulphide oxidation under partially anoxic conditions at the bed of the Haut Glacier d'Arolla, Switzerland." Hydrological Processes 16: 2363-2368.

Brody, J. R., Kern S.E. (2004). "Sodium boric acid: a Tris-free, cooler conductive medium for DNA electrophoresis." BioTechniques 36: 214-216.

Brown, G.H.; Sharp, M.J.; Tranter, M.; Gurnell, A.M.; Nienow, P.W. (1994). "Impact of post-mixing chemical reactions on the major ion chemistry of bulk meltwaters draining the Haut Glacier D'Arolla, Valais, Switzerland." Hydrological Processes 8: 465-480.

Brown, G.H., Sharp, M.J., Tranter, M. (1996). "Subglacial chemical erosion: seasonal variations in solute provenance, Haut Glacier d'Arolla, Valais, Switzerland." Journal of Glaciology 22: 25-31.

Christner, B.C., Mosley-Thompson, E., Thompson, L.G., Reeve, J.N. (2001) "Isolation of bacteria and 16S rDNAs from Lake Vostok accretion ice." Environmental Microbiology 3: 570-577.

Dowdeswell, J.A., Siegert, M.J. (2002) "The physiography of modern Antarctic subglacial lakes." Global and Planetary Change 35: 221-236.

Foght, J., Aislabie, J., Turner, S., Brown, C.E., Ryburn, J., Saul, D.J., Lawson, W. (2004). "Culturable Bacteria in Subglacial Sediments and Ice from Two Southern Hemisphere Glaciers." Microbial Ecology 47: 329-340.

Fountain, A.G., Jacobel, R.W., Schlichting, R., Jansson, P. (2005). "Fractures as the main pathways of water flow in temperate glaciers." Nature 433. 618-621.

Fountain, A.G., Walder, J.S., (1998). "Water flow through temperate glaciers." Review of Geophysics 36: 299-328.

Franson, M. A. H. (1981). Standard methods for the examination of water and wastewater. Washington, D.C., American Public Health Association: 447-448.

Gaidos, E., Lanoil, B., Thorsteinsson, T., Graham, A., Skidmore, M.L., Han, Suk-Kyun, Rust, T., Popp, B., (2004) "A Viable Microbial Community in a Subglacial Volcanic Crater Lake, Iceland." Astrobiology 4: 327-344.

Gibbs, M.T., Kump, L.R. (1994). "Global chemical erosion during the last glacial maximum and the present: Sensitivity to changes in lithology and hydrology." Paleoceanography 9: 529-544.

Gordon, D. A., Giovannoni, S.J. (1996). "Detection of stratified microbial populations related to *Chlorobium* and *Fibrobacter* species in the Atlantic and Pacific oceans." Applied and Environmental Microbiology 62: 1171-1177.

Gordon, S., Sharp, M., Hubbard, B., Willis, I.C., Smart, C., Copland, L., Harbor, J., Ketterling, B. (2001). “Borehole drainage and its implications for the investigation of glacier hydrology: experiences from Haut Glacier d'Arolla, Switzerland.” Hydrological Processes 15: 797-813.

Gounot, A.M. 2001. Ecology of psychrophilic and psychrotrophic microorganisms in cold and frozen soils. In: Paepe, R. and Melnikov, V. (eds.).Permafrost Response on Economic Development, Environmental Security andNatural Resources. Proceedings of the NATO Advanced Research Workshop onPermafrost Response on Economic Development, Environmental Security and Natural Resources, Novosibirsk, Russia, 1216November 1998. p. 543-551.

Harbor, J., Sharp, M., Copland, L., Hubbard, B., Nienow, P., Mair, D. (1997). “Influence of subglacial drainage conditions on the velocity distribution within a glacier cross section.” Geology 8: 739-742

Harper, J. T., Humphrey, N.F., Pfeffer, W.T., Fudge, T., O'neel, S. (2005). “Evolution of subglacial water pressure along a glacier's length.” Annals of Glaciology 40: 1-6.

Holland, H.D. (1978). “The Chemistry of the Atmosphere and Oceans” Wiley, New York.

Holloway, J. M., Dahlgren, R.A., Hansen, B., Casey, W.H. (1998). “Contribution of bedrock nitrogen to high nitrate concentrations in stream water.” Nature 395: 785-788.

Hosein, R., Arn, K., Steinman, P., Adatte, T., Follmi, K.B. (2002). “Carbonate and silicate weathering in two presently glaciated, crystalline catchments in the Swiss Alps.” Chemical Geology :1-13.

Houghton, J.T., Ding, Y. Griggs, D.J., Noguer, M., van der Linden, P.J., Dai, X., Maskell, K. Johnson, C.A. (2001) Climate Change 2001 – the Scientific Basis. Contribution of Working Group I to the Third Assessment Report of the Intergovernmental Panel on Climate Change, Cambridge University Press, 94pp.

Hubbard, B. P., Sharp, M. J., Willis, I. C., Nielsen, M. K., Smart, C. C. (1995). “Borehole water-level variation and the structure of the subglacial hydrological system of Haut Glacier d’Arolla, Valais, Switzerland.” Journal of Glaciology 41(139): 572-583.

Kamb W.B. (1987) “Glacier surge mechanism based on linked cavity configuration of the basal water conduit system.” Journal of. Geophysical. Research. 92 (B9): pp. 9083-9100.

Karl, D.M., Bird, D.F., Björkman, K., Houlihan, T., Shackelford, R., Tupas, L. (1999) "Microorganisms in the accreted ice of Lake Vostok, Antarctica." Science 286: 2144–2147.

Kirschvink, J.L. (1992) Late Proterozoic Low-Latitude Global Glaciation: the Snowball Earth. Cambridge University Press. Cambridge, United Kingdom.

Kirchman, D. L., Sigda, J., Kapuscinski, R., Mitchell, R. (1982). "Statistical analysis of the direct count method for evaluating bacteria." Applied and Environmental Microbiology 44: 376-382.

Kivimäki, A.L. (2005). "Presence of microbial populations in glaciers and their impact on rock weathering at glacial beds." Doctoral Dissertation. University of Bristol, Department of Earth Science.

Knight, P.G. (1999) Glaciers. Nelson Thornes Ltd., Cheltenham, England

Lane, D. J. (1991). 16S, 23S rRNA sequencing. Nucleic Acid Techniques in Bacterial Systematics. eds. E. Stackebrandt and M. Goodfellow. New York, John Wiley and Sons: 115-175.

Mair, D. W. F., Sharp, M.J., Willis, I. C. (2002). "Evidence for basal cavity opening from analysis of surface uplift during a high-velocity event: Haut Glacier d'Arolla, Switzerland." Journal of Glaciology 48: 208-216.

Mitchell, A., Brown, G.H., Fuge, R. (2001). "Minor and trace element export from a glacierized Alpine headwater catchment (Haut Glacier d'Arolla, Switzerland)." Hydrological Processes **15**: 3499-3524.

Mitchell, A. C., Brown, G.H., Fuge, R. (2006). "Minor and trace elements as indicators of chemical weathering and flow routing in subglacial environements." Hydrological Processes 20: 877-897.

Muyzer, G., de Waal, E.C., Uitterlinden, A.G. (1993). "Profiling of complex microbial populations by denaturing gradient gel electrophoresis analysis of polymerase chain reaction amplified genes coding for 16S ribosomal RNA." Applied and Environmental Microbiology 59: 695-700.

Nicholson, R.V., Gillham, R.W., Reardon, E.J. (1988). "Pyrite oxidation in carbonate-buffered solution:1. Experimental Kinetics." Geochimica et Cosmochimica Acta 52: 1077-1085.

Nienow, P. W., Sharp, M., Willis, I.C. (1998). "Seasonal changes in the morphology of the subglacial drainage system, Haut Glacier d'Arolla, Switzerland." Earth Surface Processes and Landforms 23: 105-133.

Parkhurst, D.L. (1995) “User's guide to PHREEQC--A computer program for speciation, reaction-path, advective-transport, and inverse geochemical calculations:” U.S. Geological Survey Water-Resources Investigations Report 95-4227, 143 p.

Paterson, W. S. B. (1994). “The physics of glaciers”, 3rd edition. Elsevier Science Inc., Tarrytown, New York.

Porter, K. G., Feig, Y.S. (1980). “The use of DAPI for identification and counting aquatic flora.” Limnology and Oceanography 25: 943-948.

Priscu, J.C., Adams, E.E., Lyons, W.B., Voytek, M.A., Mogk, D.W., Brown, R.L., McKay, C.P., Takacs, C.D., Welch, K.A., Wolf, C.F., Kirschtein, J.D., Avci, R. (1999) “Geomicrobiology of subglacial ice above Lake Vostok, Antarctica.” Science 286: 2141–2144.

Sebilo, M., Billen, G., Grably, M., Mariotti, A. (2003). “Isotopic composition of nitrate-nitrogen as a marker of riparian and benthic denitrification at the scale of the whole Seine River.” Biogeochemistry 63(1): 35-51.

Sharp, R. P. (1988). Living Ice- Understanding Glaciers and Glaciation, Cambridge University Press: 225.

Sharp, M., Tranter, M., Brown, G.H., Skidmore, M. (1995). “Rates of chemical denudation and CO_2 drawdown in a glacier-covered alpine catchment.” Geology 23: 61-64.

Sharp, M., Parkes, J., Cragg, B., Fairchild, I.J., Lamb, H., Tranter, M. (1999). “Widespread bacterial populations at glacier beds and their relationship to rock weathering and carbon cycling.” Geology 27: 107-110.

Sharp, M., Creaser, R.A., Skidmore, M. (2002). “Strontium isotope composition of runoff from a glaciated carbonate terrain.” Geochimica et Cosmochimica Acta 66: 595-614.

Sigler, W. V., Zeyer, J. (2002). “Microbial Diversity and Acitivty along the Forefields of Two Receding Glaciers.” Microbial Ecology 43: 397-407.

Skidmore, M. L., Sharp, M.J. (1999). “Drainage behaviour of a high Arctic polythermal glacier.” Annals of Glaciology 28**:**209-215.

Skidmore, M. L., Foght, J.M., Sharp, M.J. (2000). “Microbial life beneath a High Arctic glacier.” Applied and Environmental Microbiology 66: 3214-3220.

Skidmore, M. L., Anderson, S.P., Sharp, M.J., Foght, J.M., Lanoil, B.D. (2005). "Comparison of Microbial Community Compositions of Two Subglacial Environments Reveals a Possible Role for Microbes in Chemical Weathering Processes." Applied and Environmental Microbiology 71(11): 6986-6997.

Stumm, W., Morgan, J.J.. (1996). "Aquatic Chemistry: Chemical Equilibria and Rates in Natural Waters." John Wiley and Sons, New York.

Suzuki M T, Giovannoni S J. (1996). "Bias caused by template annealing in the amplification of mixtures of 16S rRNA genes by PCR." Applied and Environmental Microbiology. 62:625–630.

Tranter, M., Brown, G.H., Raiswell, R., Sharp, M.J., Gurnell, A.M. (1993). "A conceptual model of solute acquisition by Alpine glacial meltwaters." Journal of Glaciology 39: 573–581.

Tranter M., Brown G.H., Hodson A., Gurnell A.M., Sharp M.J. (1994). "Variations in nitrate concentration of glacial runoff in Alpine and sub-Polar environments." International Association of Hydrological Sciences Publication 223: 299–311.

Tranter, M., Brown, G.H., Hodson, A.J., Gurnell, A.M. (1996) "Hydrochemistry as an indicator of subglacial drainage system structure: a comparison of alpine and sub-polar environments." Hydrological Processes 10: 541-556.

Tranter, M., Sharp, M.J., Brown, G.H., Willis, I.C., Hubbard, B.P., Nielsen, M.K., Smart, C.C., Gordon, S., Tulley, M., H.R. Lamb (1997). "Variability in the chemical composition of *in situ* subglacial meltwaters." Hydrological Processes 11: 59-77.

Tranter, M., Sharp, M.J., Lamb, H.R., Brown, G.H., Hubbard, B.P., Willis, I.C. (2002). "Geochemical weathering at the bed of Haut Glacier d'Arolla, Switzerland- a new model." Hydrological Processes 16: 959-993.

Tranter, M., Skidmore, M., Wadham, J. (2005) "Hydrological controls on microbial communities in subglacial environments." Hydrological Processes 19: 995-998.

Wadham, J.L., Bottrell, S.H., Tranter, M., Raiswell, R. (2004) "Stable isotope evidence for microbial sulphate reduction at the bed of a polythermal high Arctic glacier." Earth and Planetary Science Letters 219: 341–355.

White A. F., Blum A. E., Bullen T. D.,Vivit D. V., Schulz M., Fitzpatrick J. (1999a) "The effect of temperature on experimental and natural weathering rates of granitoid rocks." Geochimica et Cosmochimica Acta 63, 3277-3291.

White A. F., Bullen T. D., Vivit D. V., Schulz M. S. (1999b) “The role of disseminated calcite in the chemical weathering of granitoid rocks.” Geochimica et Cosmochimica Acta, 63, 1939-1953.

Zhu, F., Wang, S., Zhou, P. (2003). “*Flavobacterium xinjiangense* sp. nov. and *Flavobacterium omnivorum* sp. nov., novel psychrophiles from the China No. 1 glacier.” International Journal of Systematic and Evolutionary Microbiology 53: 853-857.

APPENDIX A

WEATHERING EXPERIMENT DATA

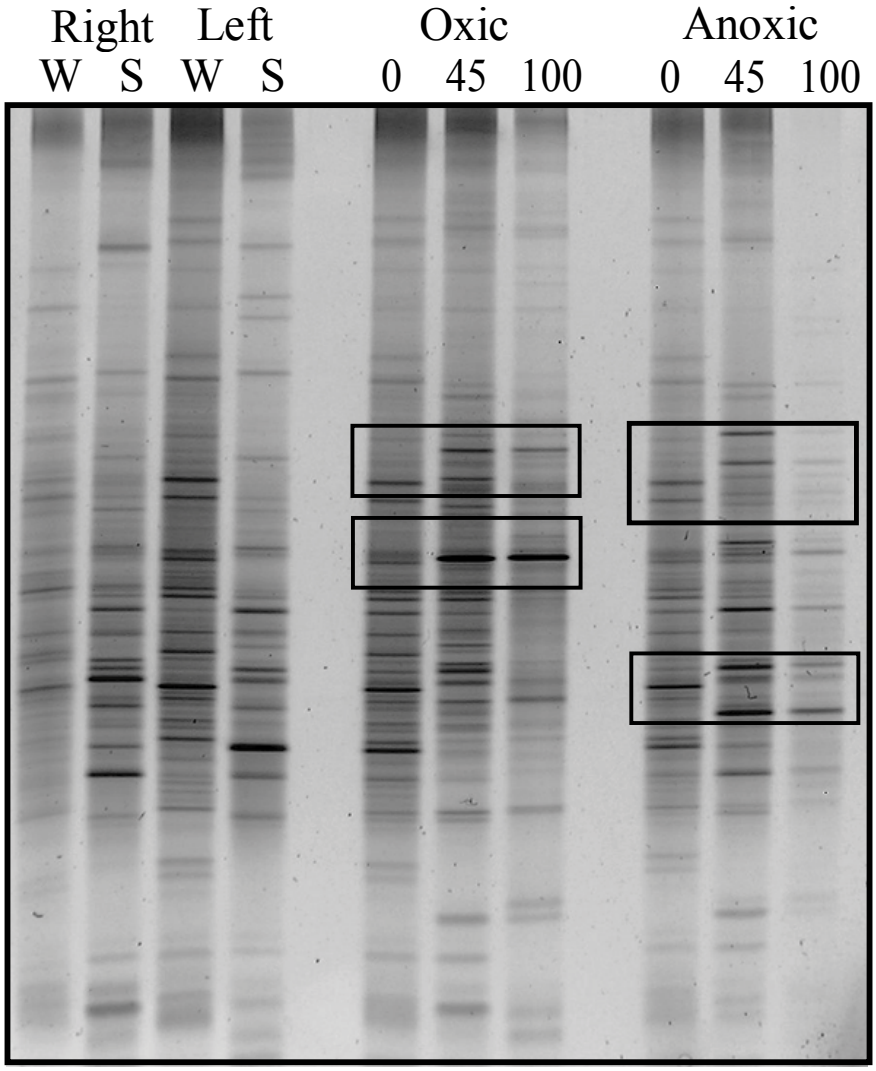

Figure A.1. DGGE profile of PCR amplified partial 16S rRNA gene sequences from field samples and sediments of live oxic and anoxic experimental bottles. Lanes 1-4 are the DGGE profiles of PCR amplified partial 16S rRNA gene sequences from meltwater (W) and sediments (S) from the right and left subglacial streams. The remaining lanes are DGGE profiles of PCR amplified partial 16S rRNA gene sequences from live oxic and anoxic sediments from days 0, 45, and 100. Changes in the DGGE profile in experimental bottles over time are highlighted by the black boxes.

Table A.1. Mean concentrations of major cations, anions, and organic acid anions in water from live and killed controls. All concentrations are in μeq L^{-1}. *HCO_3^- was calculated by charge balance using PHREEQci (Parkhurst, 1995).

Bottle	Day	pH	F^-	Cl^-	NO_3^-	PO_4^{3-}	SO_4^{2-}	*HCO_3^-	CH_3COO^-	$HCOO^-$	Na^+	NH_4^+	K^+	Ca^{2+}	Mg^{2+}
LIVE-OXIC	0	7.7	5.8	5.1	16.8	0.3	394.3	752.1	1.7	1.1	45.7	0.0	28.0	999.5	104.1
	28	7.4	6.8	5.1	0.2	0.3	401.9	1281.0	4.7	0.2	50.0	0.0	30.8	1501.7	117.6
	45	7.4	6.8	5.4	0.0	0.3	401.6	1254.5	0.3	0.4	53.5	0.0	34.3	1437.6	144.0
	60	7.4	8.7	5.1	0.0	0.3	412.3	1578.2	0.0	0.0	51.8	0.0	35.3	1782.9	134.5
	100	7.9	9.5	5.4	0.0	0.3	415.4	1929.6	0.0	0.2	57.4	0.0	42.0	2105.0	155.9
LIVE-ANOXIC	0	7.7	6.1	4.5	16.9	0.3	404.1	700.1	1.1	2.1	43.5	0.0	23.6	963.1	104.1
	28	7.1	6.8	4.5	0.2	0.6	396.8	778.0	2.1	0.3	43.1	0.0	24.0	1017.5	102.8
	45	7.1	6.8	5.1	0.0	0.3	398.1	843.4	35.4	0.4	43.9	0.0	21.1	1076.8	114.3
	60	7.4	6.8	4.8	0.0	0.3	399.1	949.1	50.0	0.2	39.2	0.0	13.7	1187.1	123.4
	100	7.7	7.4	4.2	0.0	0.3	398.3	1052.7	139.0	0.0	33.9	0.0	9.9	1296.9	130.4
DEAD (heat)- OXIC	0	7.8	7.9	7.3	16.9	0.9	400.6	667.0	2.9	2.0	75.5	0.55	64.6	908.7	56.3
	28	7.2	7.9	6.5	16.9	1.3	407.3	899.3	2.5	1.3	73.3	0.28	41.5	1149.7	78.1
	45	7.0	7.6	5.6	16.9	1.3	407.0	841.1	3.4	1.6	71.3	0.55	39.2	1100.3	73.2
	60	7.4	7.9	6.2	16.9	1.3	405.3	785.6	1.8	1.4	70.0	0.55	38.7	1039.4	77.7
	100	7.4	7.9	6.2	16.9	1.3	406.8	803.6	1.6	1.1	71.1	0.55	42.5	1053.1	78.1
DEAD (heat)- ANOXIC	0	7.3	8.4	6.1	16.8	0.9	404.7	612.0	1.9	1.6	74.8	0.55	61.4	856.3	59.2
	28	7.0	7.9	4.8	16.8	1.3	400.7	819.2	2.6	1.3	67.9	0.28	35.9	1075.3	75.3
	45	7.1	7.4	5.6	17.0	1.3	400.2	952.4	4.2	1.3	70.3	0.55	40.1	1200.8	77.7
	60	7.5	7.9	5.6	16.7	1.3	402.6	869.2	2.2	1.6	67.4	0.55	37.9	1128.7	72.4
	100	7.4	7.9	10.7	16.5	1.3	406.8	895.9	3.9	1.3	73.5	0.55	42.4	1149.7	78.1
DEAD (chemical) - OXIC	0	7.7	1.8	15.2	18.2	0.6	382.6	754.6			7.6	0.0	37.1	1110.3	121.33
	28	7.1	0.0	11.0	18.1	0.9	390.8	1152.8			7.6	0.0	45.7	1560.4	125.86
	45	7.1	1.1	13.0	18.4	1.1	387.8	1490.6			7.6	0.0	53.0	1780.4	137.37
	60	7.2	1.3	11.6	18.2	0.6	385.4	1479.2			7.4	0.0	48.9	1783.9	122.57
	100	7.1													
DEAD (chemical)- ANOXIC	0	7.8	1.6	15.2	18.8	0.6	380.3	571.0			4.1	0.0	36.3	979.5	107.8
	28	7.0	0.0	16.4	19.2	0.6	379.5	1410.1			7.4	0.0	51.2	1802.6	130.4
	45	7.1	1.1	12.1	17.7	0.6	380.2	1573.2			7.6	0.0	49.4	1850.0	150.5
	60	7.1	0.5	16.9	18.9	0.6	372.3	1720.9			7.8	0.0	54.4	1942.4	145.6
	100	7.4	0.4	2.8	18.9	0.6	372.3								

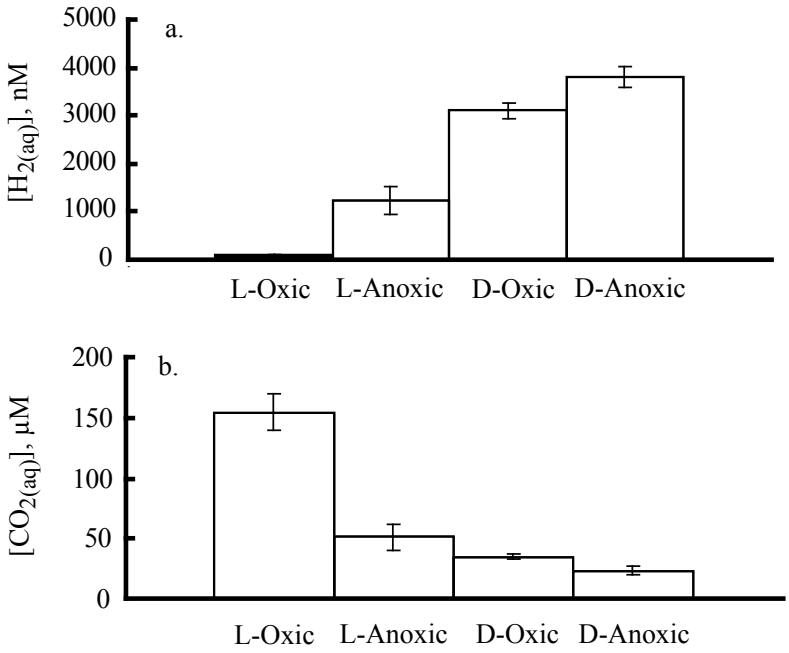

Figure A.2. Concentration of dissolved gases in live and killed control bottles at day 100. The concentration of $H_{2(aq)}$ (a.) and $CO_{2(aq)}$ (b.)in live (L) and killed control (D) bottles incubated under oxic and anoxic conditions for 100 days.

Table A.2 Live / Dead staining of bacterial cells in sediments from oxic and anoxic killed control bottles.

Bottle Treatment	Day	Live cells g^{-1} sediment *(std. dev.)*	Dead cells g^{-1} sediment *(std. dev.)*	Total cells g^{-1} sediment	Dead cells/Total cells (%)
Dead- Oxic	0	1.65E+02 *6.77E+01*	5.97E+03 *5.30E+02*	6.14E+03	97%
Dead- Oxic	100	5.05E+01 *8.88E+01*	2.83E+04 *8.88E+02*	2.84E+04	100%
Dead- Anoxic	0	7.05E+02 *4.40E+01*	9.33E+03 *4.45E+02*	1.00E+04	93%
Dead- Anoxic	100	6.17E+02 *8.90E+01*	2.10E+04 *7.44E+02*	2.17E+04	97%
Live- Oxic	100	2.64E+04 *2.16E+03*	2.60E+04 *2.07E+03*	5.24E+04	50%
	NaCl blank	0.00E+00 0.00E+00	7.60E+01 5.41E+01	7.60E+01	100%

Table A.3. Statistical analysis of the concentration of ions released into solution in live vs. killed controls over time. The slope of a line (ion concentration vs. time) was compared for ions from live and killed control bottles. The t-test results were generated using S-plus software.

Ca^{2+}	
df	4
t stat	235.6567
P(T<=t) two tail	1.95×10^{-9}

Na^{+}	
df	4
t stat	41.1768
P(T<=t) two tail	2.08×10^{-6}

Mg^{2+}	
df	4
t stat	100.3288
P(T<=t) two tail	5.92×10^{-8}

SO_4^{2-}	
df	4
t stat	6.2496
P(T<=t) two tail	3.30×10^{-3}

Table A.4 Weathering calculations from live and killed control bottles.

	Ca^{2+} (μeq L^{-1})	SO_4^{2-} (μeq L^{-1})	*HCO_3- (μeq L^{-1})	Ca/SO_4	S-ratio
Live Oxic					
Day 0	999.5	394.3	750.9	2.5	0.3
Day 100	2105.0	415.4	1926.1	5.1	0.2
Dead Oxic					
Day 0	908.7	400.6	665.9	2.3	0.6
Day 100	1053.1	406.8	800.7	2.6	0.5
Live Anoxic					
Day 0	963.1	404.1	694.3	2.4	0.4
Day 100	1296.9	398.3	1058.6	3.3	0.3
Dead Anoxic					
Day 0	856.3	404.7	608.6	2.1	0.4
Day 100	1149.7	406.8	895.4	2.8	0.3

Table A.5. Powder X-ray diffraction of sediments from live and killed control bottles. The results of XRD analysis of sediment from live and heat-sterilized sediment from day 0 and 100 are shown.

Live Oxic-0	**Live Oxic-100**	**Dead-Oxic-0**	**Dead Anoxic-100**
Quartz	Quartz	Quartz	Quartz
Albite	Albite	Albite	Albite
Anorthite	Anorthite	Anorthite	Anorthite
Orthoclase	Orthoclase	Orthoclase	Orthoclase
	Actinolite	Actinolite	Actinolite
Muscovite	Muscovite	Muscovite	Muscovite
Kaolinite	Kaolinite	Kaolinite	Kaolinite

Table A.6. Electron Dispersive Spectroscopy (EDS) of sediments (Day 0 and 100) from live oxic bottles. Nine spots were analyzed from live oxic bottles from day 0 (L0) and day 100 (L100).

	c (% atoms)							
Sample	Ca	O	Fe	Na	Mg	Al	Si	K
L0-1	0.09	36.05	0.18	0.44	0.12	1.14	4.09	0.25
L0-2	0.07	74.87	0.07	4.04	0.13	5.33	15.24	0.26
L0-3	0.06	72.54	1.33	2.74	1.35	6.49	14.86	0.63
L0-4	0.00	83.01	0.00	0.00	0.00	0.01	16.97	0.00
L0-5	0.04	67.11	0.47	4.94	0.51	6.55	19.90	0.49
L0-6	0.06	72.54	1.33	2.74	1.35	6.49	14.86	0.63
L0-7	0.00	83.01	0.00	0.00	0.00	0.01	16.97	0.00
L0-8	0.04	67.11	0.47	4.94	0.51	6.55	19.90	0.49
L0-9	0.20	67.21	0.29	1.43	0.37	8.65	18.74	3.11
L100-1	0.07	76.74	0.08	0.22	0.10	0.79	21.81	0.20
L100-2	0.04	73.59	0.02	4.57	0.08	5.66	15.96	0.08
L100-3	0.20	67.21	0.29	1.43	0.37	8.65	18.74	3.11
L100-4	0.23	41.96	16.97	8.58	0.96	8.64	20.87	1.79
L100-5	0.07	66.10	1.47	0.01	1.47	9.32	16.67	4.88
L100-6	0.08	67.30	0.10	0.95	0.16	7.06	19.31	5.04
L100-7	0.07	74.87	0.07	4.04	0.13	5.33	15.24	0.26
L100-8	0.06	64.95	8.59	0.15	7.47	7.50	11.19	0.08
L100-9	2.39	79.96	2.32	0.14	0.01	4.10	9.73	1.37